Recursive State Machine Guided Graph Folding for Context-Free Language Reachability

YUXIANG LEI, University of New South Wales, Australia
YULEI SUI, University of New South Wales, Australia
SHIN HWEI TAN, Concordia University, Canada
QIRUN ZHANG, Georgia Institute of Technology, USA

Context-free language reachability (CFL-reachability) is a fundamental framework for program analysis. A large variety of static analyses can be formulated as CFL-reachability problems, which determines whether specific source-sink pairs in an edge-labeled graph are connected by a reachable path, *i.e.*, a path whose edge labels form a string accepted by the given CFL. Computing CFL-reachability is expensive. The fastest algorithm exhibits a slightly subcubic time complexity with respect to the input graph size. Improving the scalability of CFL-reachability is of practical interest, but reducing the time complexity is inherently difficult.

In this paper, we focus on improving the scalability of CFL-reachability from a more practical perspective—reducing the input graph size. Our idea arises from the existence of trivial edges, *i.e.*, edges that do not affect any reachable path in CFL-reachability. We observe that two nodes joined by trivial edges can be *folded*—by merging the two nodes with all the edges joining them removed—without affecting the CFL-reachability result. By studying the characteristic of the recursive state machines (RSMs), an alternative form of CFLs, we propose an approach to identify foldable node pairs without the need to verify the underlying reachable paths (which is equivalent to solving the CFL-reachability problem). In particular, given a CFL-reachability problem instance with an input graph G and an RSM, based on the correspondence between paths in G and state transitions in RSM, we propose a *graph folding principle*, which can determine whether two adjacent nodes are foldable by examining only their incoming and outgoing edges.

On top of the graph folding principle, we propose an efficient *graph folding algorithm* Gf. The time complexity of Gf is linear with respect to the number of nodes in the input graph. Our evaluations on two clients (alias analysis and value-flow analysis) show that Gf significantly accelerates RSM/CFL-reachability by reducing the input graph size. On average, for value-flow analysis, Gf reduces 60.96% of nodes and 42.67% of edges of the input graphs, obtaining a speedup of 4.65× and a memory usage reduction of 57.35%. For alias analysis, Gf reduces 38.93% of nodes and 35.61% of edges of the input graphs, obtaining a speedup of 3.21× and a memory usage reduction of 65.19%.

CCS Concepts: • **Theory of computation → Grammars and context-free languages**.

Additional Key Words and Phrases: CFL-reachability, recursive state machines, graph simplification

ACM Reference Format:
Yuxiang Lei, Yulei Sui, Shin Hwei Tan, and Qirun Zhang. 2023. Recursive State Machine Guided Graph Folding for Context-Free Language Reachability. *Proc. ACM Program. Lang.* 7, PLDI, Article 119 (June 2023), 25 pages. https://doi.org/10.1145/3591233

Authors' addresses: Yuxiang Lei, yuxiang.lei@unsw.edu.au, University of New South Wales, Australia; Yulei Sui, y.sui@unsw.edu.au, University of New South Wales, Australia; Shin Hwei Tan, shinhwei.tan@concordia.ca, Concordia University, Canada; Qirun Zhang, qrzhang@gatech.edu, Georgia Institute of Technology, USA.

Permission to make digital or hard copies of part or all of this work for personal or classroom use is granted without fee provided that copies are not made or distributed for profit or commercial advantage and that copies bear this notice and the full citation on the first page. Copyrights for third-party components of this work must be honored. For all other uses, contact the owner/author(s).
© 2023 Copyright held by the owner/author(s).
2475-1421/2023/6-ART119
https://doi.org/10.1145/3591233

1 INTRODUCTION

Context-free language reachability (CFL-reachability) [Reps 1998], also extensively studied in an alternative form called recursive state machine reachability (RSM-reachability) [Alur et al. 2005a], is a fundamental framework for program analysis. A large variety of static analyses, such as dataflow analysis [Reps et al. 1995], polymorphic flow analysis [Rehof and Fähndrich 2001], typestate analysis [Naeem and Lhoták 2008], code embedding [Sui et al. 2020] and point-to analysis [Zheng and Rugina 2008] can be formulated as CFL-reachability problems, which determine whether specific source-sink pairs in an edge-labeled graph can be connected by a path whose edge labels form a string accepted by the given CFL.

Unfortunately, solving RSM-reachability is quite expensive. The standard algorithm [Melski and Reps 2000; Reps et al. 1995] exhibits a cubic time complexity with respect to the input graph size. Improving the time complexity of CFL-reachability is inherently difficult. Due to Chatterjee et al. [2018], the truly subcubic $O(n^{3-\epsilon})$ bounds of CFL-reachability cannot be obtained without obtaining $O(n^{3-\epsilon})$-time combinatorial algorithms for Boolean Matrix Multiplication [Williams and Williams 2018]. In the literature, asymptotically faster algorithms are known only on restricted context-free languages, *i.e.*, bidirected Dyck-reachability [Chatterjee et al. 2018; Zhang et al. 2013].

Instead of reducing the (slightly) subcubic complexity, we focus on improving the scalability from a more practical perspective—reducing the size of input graphs. In the context of CFL-reachability (and its alternative forms such as set-constraint [Melski and Reps 2000]), several graph simplification techniques have been proposed: (1) The most popular technique is *cycle elimination* [Fähndrich et al. 1998; Hardekopf and Lin 2007a; Lei and Sui 2019; Pereira and Berlin 2009]. However, there is no general cycle elimination algorithm for CFL-reachability because whether a cycle can be collapsed depends on the context-free grammar (CFG). Moreover, our empirical results (Section 6) show that there are still a large number of collapsible nodes and edges, which do not reside in cycles; (2) Recently, a graph simplification algorithm [Li et al. 2020] was proposed to remove particular "non-Dyck-contributing" parenthesis-labeled edges for problems where the underlying CFL over-approximates the intersection of multiple Dyck languages (*i.e.*, the InterDyck language). Nevertheless, there are a variety of problems where the parenthesis-labeled edges do not dominate [Naeem and Lhoták 2008; Sui and Xue 2016a; Zheng and Rugina 2008], whereby the effectiveness of the InterDyck graph simplification algorithm compromises; and (3) *Edge contraction* for particular clients has also been studied. The best-known method is the offline variable substitution for pointer analysis [Rountev and Chandra 2000], a special case of the more general graph folding problem.

In this paper, we introduce a novel *graph folding technique for CFL-reachability*. The graph folding technique extends the applicability of edge contraction from the special case [Rountev and Chandra 2000] to general CFL-reachability. The foldability of CFL-reachability originates from the existence of *trivial edges*. If two nodes are joined by trivial edges, they can be folded—by merging the two nodes and removing all the edges joining them—without affecting the CFL-reachability result.

The challenge lies in identifying foldable node pairs. Intuitively, we can identify the foldable node pairs by determining all reachable paths. However, this is equivalent to solving CFL-reachability and obviously defeats the purpose of improving scalability. In this paper, we utilize an equivalent form of CFLs called recursive state machines (RSMs) and address the challenge for problems where the CFLs can be expressed as *deterministic* RSMs. In deterministic RSMs, each target state can be uniquely determined by the source state and the transition label. Therefore, our key technical insight is to study the correspondence between paths in graphs and state transition chains in deterministic RSMs, and refine the criteria for foldable node pairs. In particular, we consider a node pair (x, y) as *foldable* if the corresponding RSM transitions of each path in the graph are consistent before and after folding (x, y). By further exploiting the dependency of RSM state transitions, we

introduce a graph folding principle for deterministic RSMs, which can identify foldable node pairs by examining only their incoming and outgoing edges in the input graph.

On top of the graph folding principle, we propose a graph-folding algorithm Gf, which has a linear time complexity with respect to the number of nodes in the input graph. Gf enables a general preprocessing step for CFL/RSM-reachability where the RSM is deterministic. Deterministic RSMs cover a large variety of languages extensively used in program analysis, including visibly pushdown languages [Alur and Madhusudan 2004], Dyck languages [Kodumal and Aiken 2004], and all regular languages. By reducing the input graph size, graph folding significantly improves the scalability of CFL-reachability in terms of both time and space.

We have implemented Gf and applied it to a context-sensitive value-flow analysis [Sui and Xue 2018; Sui et al. 2014], and a field-sensitive alias analysis [Zheng and Rugina 2008]. We have extensively evaluated it using benchmarks of ten popular GitHub projects in C/C++. Our experimental results show that Gf can significantly reduce the graph sizes for the two client analyses. In general, by reducing 60.96% nodes and 42.67% edges of the input graphs, Gf accelerates context-sensitive value-flow analysis by 4.65× with a memory reduction rate of 57.35%; by reducing 38.93% nodes and 35.61% edges, Gf accelerates field-sensitive alias analysis by 3.21× with a memory reduction rate of 65.19%. The performance of Gf in both clients surpasses existing graph simplification techniques [Li et al. 2020; Nuutila and Soisalon-Soininen 1994].

This paper makes the following contributions:

(1) We introduce a new perspective that utilizes deterministic RSMs to simplify the input graphs of CFL-reachability.
(2) For deterministic CFL- and RSM-reachability, we propose a graph folding principle that identifies foldable node pairs by examining only their incoming and outgoing edges in the input graph.
(3) We propose an efficient graph-folding algorithm Gf, whose time complexity is linear with respect to the number of nodes of the input graph.
(4) We apply Gf to a context-sensitive value-flow analysis and a field-sensitive alias analysis on ten open-source C/C++ programs. The results demonstrate that graph folding significantly reduces running time and memory overhead by reducing the input graph size.

The remainder of this paper is organized as follows: Section 2 presents a motivating example. Section 3 introduces the background and formulates graph folding. Section 4 studies the criteria for foldable node pairs. Section 5 proposes our graph-folding algorithm Gf, followed by experiments in Section 6, and related work and conclusion in Sections 7 and 8, respectively.

2 MOTIVATING EXAMPLE

This section motivates graph folding for CFL-reachability, describing the benefits and challenges. Figure 1(a) shows a CFG of a Dyck language variant and its corresponding RSM. Let S be the start symbol of the CFG in Figure 1(a). This grammar generates a Dyck language of matched parentheses "$(\!|$" and "$|\!)$" with an arbitrary number of "a"s. Dyck languages are widely used in context-sensitive program analyses [Hao et al. 2015; Heine and Lam 2003; Reps et al. 1995; Zhang and Su 2017]. In this motivating example, we focus on the reachability problem that identifies S-reachable node pairs starting with v_0 and v_1. Figure 1(b) gives the input graph G. In G, there are four S-reachable node pairs (v_0, v_7), (v_1, v_5), (v_1, v_6) and (v_1, v_7). Figure 1(c) gives the details of the S-reachable node pairs and the corresponding S-paths, where the column "String" contains the corresponding path strings. Note that there is no cycle in G, and removing any parenthesis-labeled edge changes the CFL-reachability solution. Hence, neither cycle elimination [Nuutila and Soisalon-Soininen 1994] nor InterDyck graph simplification [Li et al. 2020] can simply G in this example.

CFG: $S = (\ S\ ) \mid S\ S \mid a^*$

RSM: M_1

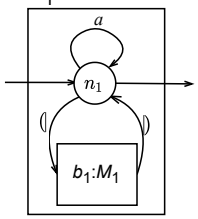

(a) A context-free grammar and its equivalent recursive state machine.

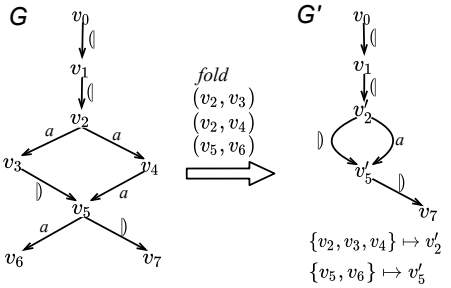

(b) Original input graph G and the transformed graph G' via graph folding.

Solution	Reachable path	String
(v_0, v_7)	$v_0 \xrightarrow{(} v_1 \xrightarrow{(} v_2 \xrightarrow{a} v_3 \xrightarrow{)} v_5 \xrightarrow{)} v_7$	$(\ (\ a\ )\ )$
(v_1, v_5)	$v_1 \xrightarrow{(} v_2 \xrightarrow{a} v_3 \xrightarrow{)} v_5$	$(\ a\ )$
(v_1, v_6)	$v_1 \xrightarrow{(} v_2 \xrightarrow{a} v_3 \xrightarrow{)} v_5 \xrightarrow{a} v_6$	$(\ a\ )a$
(v_1, v_7)	$v_1 \xrightarrow{(} v_2 \xrightarrow{a} v_4 \xrightarrow{a} v_5 \xrightarrow{)} v_7$	$(\ aa\ )$

(c) Reachability solutions in G.

Solution	Reachable path	String
(v_0, v_7)	$v_0 \xrightarrow{(} v_1 \xrightarrow{(} v'_2 \xrightarrow{)} v'_5 \xrightarrow{)} v_7$	$(\ (\ )\ )$
(v_1, v'_5)	$v_1 \xrightarrow{(} v'_2 \xrightarrow{)} v'_5$	$(\ )$
(v_1, v_7)	$v_1 \xrightarrow{(} v'_2 \xrightarrow{a} v'_5 \xrightarrow{)} v_7$	$(\ a\ )$

(d) Reachability solutions in G'.

Fig. 1. Motivating example for graph folding.

Graph Folding. Graph folding reduces the graph size by merging adjacent node pairs and removing the corresponding edges. Most importantly, it does not affect the original reachability result. Figure 1(b) gives the folded graph G' from G. Specifically, the node pair (v_2, v_3) is folded into a representative node v'_2 with $v_2 \xrightarrow{a} v_3$ removed. Likewise, (v_2, v_4) and (v_5, v_6) are folded into v'_2 and v'_5, respectively. Figure 1(d) gives the reachability result on G'. Notably, v'_5 in G' represents nodes v_5 and v_6 in G. By expanding v'_5 in (v_1, v'_5) back into v_5 and v_6, we get two S-reachable pairs (v_1, v_5) and (v_1, v_6). As a result, the reachability results from G' and G are the same. Hence, graph folding can reduce the size of G while maintaining the correctness of the solution.

Benefits. Proper preprocessing that shrinks the input graph can significantly reduce the computation overhead for CFL-reachability. Given a graph G, standard CFL-reachability algorithm [Melski and Reps 2000] takes cubic time with respect to the number of nodes in G. Specifically, in Figure 1(b), there are eight nodes and eight edges in the original graph G. Assume that each iteration inserts a summary edge into the graph. Then, performing the standard CFL-reachability algorithm upon G costs 23 iterations. In contrast, there are only five nodes and five edges in the folded graph G', which only costs 13 iterations to obtain the result. By reducing the graph size, graph folding can reduce 43.48% of iterations. Moreover, our graph-folding algorithm Gf has a linear time complexity with respect to the number of nodes in the graph, which is asymptotically faster than any CFL-reachability algorithm. Specifically, Gf folds the graph G in the motivating example in eight iterations. Even if we take Gf running time into account, the overall computation overhead is smaller than that without any preprocessing.

Challenge. Identifying foldable node pairs is the main technical challenge of graph folding. From the motivating example in Figure 1, we can see that we cannot fold arbitrary node pairs

in G. Consider the node pair (v_3, v_5). If we fold the pair into a representative node v_3', the path $v_1 \xrightarrow{(} v_2 \xrightarrow{a} v_3 \xrightarrow{)} v_5$ changes to $v_1 \xrightarrow{(} v_2 \xrightarrow{a} v_3'$, where v_3' represents $\{v_3, v_5\}$. Unfortunately, after this folding, the reachable pair (v_1, v_5) is missing, and cannot be retrieved from the result by expanding v_3' into v_3 and v_5. This makes the analysis unsound. In fact, it is difficult to identify all the foldable node pairs unless we identify all reachable paths first. Our key insight is to exploit the correspondence between paths in the graph and state transitions in the RSM and identify the majority of foldable node pairs. Section 4 details how to address this challenge based on the characteristics of deterministic RSMs.

3 PROBLEM FORMULATION

Context-free languages can be described using recursive state machines (RSMs) and pushdown automata (PDA). We describe graph folding in the context of RSM-reachability [Alur et al. 2005a; Chaudhuri 2008]. RSMs model stack push/pop operations in PDA using call/return state transitions. When discussing graph reachability, this makes the correspondence between paths in the graph and transition chains in RSMs more intuitive. For instance, a labeled edge $v_1 \xrightarrow{t} v_2$ in the input graph can be directly mapped to a state transition $s_1 \xrightarrow{t} s_2$ in the RSM, where s_1 and s_2 are two RSM states. This section introduces the preliminaries and formulates the problem.

3.1 Recursive State Machines

A recursive state machine (RSM) [Alur et al. 2005a] over a finite alphabet Σ is defined as a tuple $R = \langle M_1, \cdots, M_t \rangle$ comprised of t component finite state machines, where each component $M_i = \langle N_i, B_i, Y_i, En_i, Ex_i, \delta_i \rangle$ is a finite state machine consisting of the following:

N_i	– a finite set of local states.
B_i	– a finite set of boxes in M_i, with each of which mapped to a component state machine.
Y_i	$: B_i \mapsto \{1, \cdots, t\}$ – a mapping function assigning each box of M_i an index of one of the components $M_1, \cdots, M_t$.
En_i	$\subseteq N_i$ – a set holding the entries of M_i.
Ex_i	$\subseteq N_i$ – a set holding the exits of M_i.
δ_i	$: \left(N_i \cup \bigcup_{b \in B_i} Ex_{Y_i(b)}\right) \times \Sigma \mapsto N_i \cup \bigcup_{b \in B_i} En_{Y_i(b)}$ – a local transition function that maps specific states and labels to specific target states.

Specifically, for a local transition in δ_i, denoted by $n_{i_1} \xrightarrow{\ell} n_{i_2}$, (1) the source n_{i_1} must be either a local state or an exit of a box belonging in M_i, (2) the label ℓ is an element of Σ, and (3) the target n_{i_2} must be either a local state or an entry of a box in M_i.

Example 3.1. Figure 1(a) gives an example RSM over an alphabet $\Sigma = \{(, a,)\}$. There is only one component M_1 calling itself recursively. M_1 is comprised of: (1) a local state n_1, which is also the entry and the exit of M_1; (2) a box b_1 which is mapped to M_1; and (3) three transition rules $n_1 \xrightarrow{(} \langle b_1, n_1 \rangle$, $n_1 \xrightarrow{a} n_1$ and $\langle b_1, n_1 \rangle \xrightarrow{)} n_1$ where $\langle b_1, n_1 \rangle$ denotes the entry (also the exit) of the box b_1, as the labeled edges in Figure 1(a).

The semantics of RSM is given by global states and transitions:

Global states. A global state $s \in S$, where $S = B^* \times N$, $B = \bigcup_i B_i$, $N = \bigcup_i N_i$, can be viewed as a local state nested in layers of boxes. Consider a sequence of boxes $b_1, \cdots, b_k$ such that $b_i \in B_{j_i}$ and $B_{j_i}, B_{j_{i+1}} \in B$ for all $i \in \{1, \cdots, k\}$. A global state $s = \langle b_1, \cdots, b_k, n \rangle$ follows (1) $Y_{j_i}(b_i) = j_{i+1}$ for all $i \in \{1, \cdots, k\}$, *i.e.*, b_{i+1} is nested in b_i, and (2) $n \in N_{j_{k+1}}$, *i.e.*, n is nested in b_k. Intuitively, a global

state denotes the current position of the initial state (usually not nested in any box) after a series of transitions, including entering/exiting boxes.

Global transitions Δ. The global transition function $\Delta : S \times \Sigma \mapsto S$ maps specific global states and labels to specific target global states. A global transition rule is denoted by $s_1 \xrightarrow{\ell} s_2 \in \Delta$, where $s_1, s_2 \in S$ and $\ell \in \Sigma$. Global transitions are restricted by the local transition rules. Given two global states $s_1, s_2 \in S$ and $s_1 = \langle b_1, \cdots, b_{k-1}, b_k, n_1 \rangle$ where $b_k \in B_{j_k}$, $Y_{j_k}(b_k) = j_{k+1}$ and $n_1 \in N_{j_{k+1}}$, $s_1 \xrightarrow{\ell} s_2 \in R$ iff one of the following four situations holds:

(1) Location transition: $s_2 = \langle b_1, \cdots, b_{k-1}, b_k, n_2 \rangle$ and $n_1 \xrightarrow{\ell} n_2 \in \delta_{j_{k+1}}$;
(2) Entering a box: $s_2 = \langle b_1, \cdots, b_{k-1}, b_k, b_{k+1}, n_2 \rangle$, $b_{k+1} \in B_{k+1}$, $n_2 \in En_{Y_{j_{k+1}}(b_{k+1})}$ and $n_1 \xrightarrow{\ell} \langle b_{k+1}, n_2 \rangle \in \delta_{j_{k+1}}$;
(3) Existing from a box: $s_2 = \langle b_1, \cdots, b_{k-1}, n_2 \rangle$, $n_1 \in Ex_{j_{k+1}}$ and $\langle b_k, n_1 \rangle \xrightarrow{\ell} n_2 \in \delta_{j_k}$;
(4) Transiting across two boxes: $s_2 = \langle b_1, \cdots, b_{k-1}, b'_k, n_2 \rangle$, $n_1 \in Ex_{j_{k+1}}$, $b'_k \in B_{j_k}$, $n_2 \in En_{Y_{j_k}(b'_k)}$ and $\langle b_k, n_1 \rangle \xrightarrow{\ell} \langle b'_k, n_2 \rangle \in \delta_{j_k}$.

Property 3.1 (*Dependency of Global Transitions on Local Transitions*). A global transition can only change the innermost box (by entering/exiting) and the innermost local state (by the local transition function of the component state machine, to which the innermost box maps) of a global state.

For brevity, we refer to all the states and transitions as the global ones unless otherwise specified.

Deterministic RSMs. In a deterministic RSM R, given a state s_i and a label t, if $\exists s_i \xrightarrow{\ell} s_j \in R$, s_j is unique. In other words, for the transition function of a deterministic RSM, when the input state and label are specified, we can always determine the output state. In the remaining sections, all demonstrations and conclusions are based on deterministic RSMs.

Transition Chains. In an RSM R, a transition chain $p_R \in R$ from a source state s_0 to a target state s_k is a sequence of global transitions $s_0 \xrightarrow{\ell_1} s_1 \xrightarrow{\ell_2} \cdots \xrightarrow{\ell_k} s_k$ such that $s_{i-1} \xrightarrow{\ell_i} s_i \in \Delta$ for all $i \in \{1, \cdots, k\}$. In a deterministic RSM, given a source state s_0 and a sequence of label $\ell_1, \cdots, \ell_k$, the transition chain $s_0 \xrightarrow{\ell_1} s_1 \xrightarrow{\ell_2} \cdots \xrightarrow{\ell_k} s_k \in R$ is unique if it exists.

Acceptable Strings. Given an RSM R with a specified initial state $s_{init} \in S$ and a set of accepting states $F \subseteq S$, a string $w \in \Sigma^*$ is accepted by R iff it takes a transition chain from the initial state to one of the accepting states, *i.e.*, $\exists\, s_{init} \xrightarrow{\ell_1} \cdots \xrightarrow{\ell_k} s_k \in R$ such that $s_k \in F$ and $\ell_1 \cdots \ell_k = w$.

3.2 RSM-Reachability

Given a source-sink node pair, RSM-reachability is to check whether the sink is reachable from the source by a path whose edge labels form, in sequence, an acceptable string of the RSM.

Reachable Paths and Pairs. Given an RSM-reachability instance $Reach\langle R, G \rangle$ where R is an RSM and $G = \langle V, E \rangle$ is an edge-labeled directed graph, a path $p_G = v_i \xrightarrow{\ell_1} \cdots \xrightarrow{\ell_k} v_j \in G$ is a reachable path iff the sequence of the edge labels $\ell_1 \cdots \ell_k$ forms an acceptable string of R. In an RSM-reachability instance, a reachable pair $(v_i, v_j) \in V \times V$ is a node pair in G such that there exists at least one reachable path from v_i to v_j.

RSM-reachability. Formally, given an RSM R with a specified initial state and accepting states and a graph G with specified sources $V_{src} \subseteq V$ and sinks $V_{snk} \subseteq V$, an RSM-reachability problem aims to determine for each source-sink pair $(v_i, v_j) \in V_{src} \times V_{snk}$ whether it is a reachable pair.

Example 3.2. We formulate the motivating example (Figure 1) as an RSM-reachability problem. In this instance, $R = \langle M_1 \rangle$, $s_{init} = \langle n_1 \rangle$, $F = \{\langle n_1 \rangle\}$, $V_{src} = \{v_0, v_1\}$, $V_{snk} = \{v_0, \cdots, v_7\}$. For the path $v_1 \xrightarrow{(} v_2 \xrightarrow{a} v_3 \xrightarrow{)} v_5 \in G$, the sequence of edge labels forms a string "$(\ a\ )$" which is accepted by R because there is a transition chain $\langle n_1 \rangle \xrightarrow{(} \langle b_1, n_1 \rangle \xrightarrow{a} \langle b_1, n_1 \rangle \xrightarrow{)} \langle n_1 \rangle \in R$. Therefore, (v_1, v_5) is a reachable pair. Similarly, (v_0, v_7), (v_1, v_6) and (v_1, v_7) are also reachable pairs.

3.3 Graph Folding

Given a directed graph G and two adjacent nodes $(x, y) \in V \times V$, an *xy-folded graph* G' is constructed by removing all the edges joining x and y and collapsing (x, y) into a *representative node* z such that $Rep(x) = Rep(y) = z$. In particular, for a node $v_i \in V$, if v_i is merged into another node z, $Rep(v_i) = z$, otherwise, $Rep(v_i) = v_i$.

Intuitively, an ideal graph folding approach should fold as many node pairs as possible. However, arbitrarily folding node pairs can change reachable pairs due to removals or additions of graph edges, resulting in an incorrect RSM-reachability solution. A correct graph folding approach must guarantee the equivalence of reachable pairs in the original graph and the folded graph (Definition 3.1).

Definition 3.1 (*Reachability Equivalence*)**.** Let $G = \langle V, E \rangle$ be the original graph with V_{src} and V_{snk} specified, and let $G' = \langle V', E' \rangle$ be the folded graph, G and G' are reachability equivalent iff $\forall (v_i, v_j) \in V_{src} \times V_{snk}$, v_j is reachable from v_i in G iff $Rep(v_j)$ is reachable from $Rep(v_i)$ in G'.

Definition 3.1 implies that a correct graph folding preserves the information of all the original reachable pairs. In other words, two graphs being reachability equivalent yields equivalent RSM-reachability solutions. If folding a node pair (x, y) preserves reachability equivalence, we say that (x, y) is *foldable*.

Example 3.3. Let us revisit the motivating example in Figure 1(b). After folding the node pair $(v_2, v_3) \in G$ into $v_2' \in G'$, the reachable path $v_1 \xrightarrow{(} v_2 \xrightarrow{a} v_3 \xrightarrow{)} v_5$ becomes $v_1 \xrightarrow{(} v_2' \xrightarrow{)} v_5$, whose edge labels also form an acceptable string of the RSM. Thus, the reachable pair (v_1, v_5) is preserved after the folding. It can be computed that other reachable pairs in the original graph are also preserved. Therefore, (v_2, v_3) is foldable. In contrary, (v_3, v_5) is not foldable. If we were to fold (v_3, v_5) into v_3', the path $v_1 \xrightarrow{(} v_2 \xrightarrow{a} v_3 \xrightarrow{)} v_5$ would become $v_1 \xrightarrow{(} v_2 \xrightarrow{a} v_3'$ where v_3' represents v_3 and v_5, which is no longer a reachable path. Moreover, as there is no other reachable path from v_1 to v_3' in the folded graph, (v_1, v_3') is not a reachable pair, indicating that the original reachable pair (v_1, v_5) in G is lost in the folded graph.

Finally, we formulate our graph folding problem as follows.

> Given an RSM-reachability instance $Reach\langle R, G \rangle$, generate a smaller graph G' by folding node pairs in G and guarantee that G and G' are reachability equivalent.

4 PRINCIPLE FOR GRAPH FOLDING

Identifying foldable node pairs based on Definition 3.1 requires computing all reachable paths in the original graph G and the folded graph G', which contradicts the goal of improving scalability for RSM-reachability. In this section, we study the correspondence between nodes in the graph and states in the RSM. Specifically, we show that when folding a node pair (x, y), whether reachability equivalence is preserved can be determined by at most two transitions, starting with the

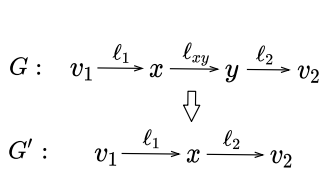

(a) When x and y are joined by only one edge, each path passing through x and y is folded into a distinct path after folding (x, y).

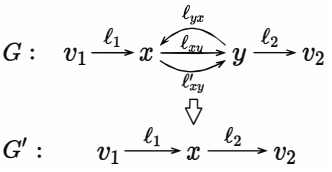

(b) When x and y are joined by multiple edges, there are multiple paths folded into the same path after folding (x, y).

Fig. 2. Correspondence between paths before and after folding. Without loss of generality, we assume that y in G is merged into x in the xy-folded graph G'.

corresponding states of x and y and going through the edge labels involving x and y. We formulate our folding principle by overapproximating the corresponding states of x and y and exploiting RSM properties, *i.e.*, the subsumption and equivalence relations of states. Thus, we can efficiently identify whether a node pair is foldable by examining only its incoming and outgoing edges.

4.1 Correspondence between Graph Folding and RSM-Reachability

Folding-Equivalent Class and Criteria for Reachability Equivalence. Consider Figure 2(a). The path $p_{G'}$ is obtained from p_G by folding (x, y), *i.e.*, contracting the edge $x \xrightarrow{\ell_{xy}} y$. In fact, the input graph in RSM-reachability can be a multigraph, meaning that there can be multiple edges between x and y, as shown in Figure 2(b). As folding (x, y) removes all the edges joining x and y, there can be multiple original paths folded into the same *xy-folded path*. Such paths in the original graph G constitute folding-equivalent classes based on their endpoints:

Definition 4.1 (*xy-Folding-Equivalent Classes*)**.** Two paths $p_1, p_2 \in G$ are in the xy-folding-equivalent (xy-FEQ) class $\boldsymbol{P}_{xy}$ iff they have identical endpoints and are folded into the same path p' in the xy-folded graph G'. A path is xy-FEQ to itself.

In Figure 2(b), all the paths starting with v_1 and ending with v_2 are in the xy-FEQ class. Based on xy-folded paths and their corresponding xy-FEQ classes, we state sufficient conditions for graph folding that can guarantee reachability equivalence in Definition 4.2. Note that our sufficient conditions do not rely on obtaining all reachable node pairs.

Definition 4.2 (*Sufficient Conditions for Reachability Equivalence*)**.** An xy-folded graph G' is reachability equivalent to its original graph G if the following conditions are satisfied:

Cond. 1. Exclusiveness: Each source-sink path in G' has a corresponding xy-FEQ class in G.
Cond. 2. Consistency: For each xy-FEQ class $\boldsymbol{P}_{xy}$ in G, its corresponding xy-folded path in G' is a reachable path iff $\boldsymbol{P}_{xy}$ contains a reachable path in G.

Satisfying the exclusiveness condition (*Cond. 1*) is straightforward. For example, we can avoid introducing extra source-sink paths to G' by not merging (x, y) when (1) there is no edge from y to x and (2) y is a source or y has incoming edges not from x. To satisfy the consistency condition (*Cond. 2*), we need to check the corresponding transition chains of reachable paths.

Corresponding Transition Chains and Corresponding States. As discussed in Section 3.1, given a specific initial state s_{init} and a string of labels $\ell_1 \cdots \ell_k$, a deterministic RSM has at most one transition chain from s_{init}, through $\ell_1 \cdots \ell_k$, to a deterministic target state s_k. Notably, the corresponding transition chain is defined below:

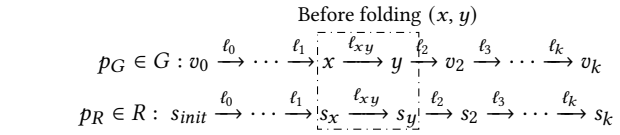

(a) A path p_G in G and its corresponding transition chain p_R in the RSM R.

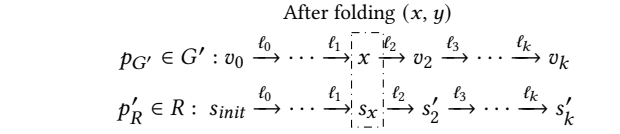

(b) The xy-folded path $p_{G'}$ of p_G and its corresponding transition chain p'_R.

Fig. 3. A path p_G and its corresponding transition chain p_R before and after folding (x, y). Without loss of generality, we assume that y is merged into x in the xy-folded graph.

Definition 4.3 (*Corresponding Transition Chain*)**.** Given an RSM-reachability instance $Reach\langle R, G\rangle$ where R is deterministic, consider a path $p_G = v_0 \xrightarrow{\ell_1} \cdots \xrightarrow{\ell_k} v_k \in G$ where $\ell_1 \cdots \ell_k$ forms a string $w \in \Sigma^k$. If there exists $p_R = s_{init} \xrightarrow{\ell_1} \cdots \xrightarrow{\ell_k} s_k \in R$ such that $\ell_1 \cdots \ell_k = w$, we say that p_R is the corresponding transition chain of p_G. As p_R, if it exists, is unique in the deterministic RSM R, a path $p_G \in G$ has zero or one corresponding transition chain.

Figure 3(a) shows a path p_G and its corresponding transition chain p_R. Similarly, Figure 3(b) depicts an xy-folded path $p_{G'} \in G'$ which has zero or one corresponding transition chain $p'_R \in R$. As depicted in Figure 3(a), with respect to the corresponding transition chain, each node v_i of a path $p_G \in G$ is mapped to exactly one state s_i in the RSM. We call s_i the corresponding state of v_i in p_G. In a graph, a node v_i may belong to multiple paths corresponding to different transition chains, leading to the notion of *corresponding states*:

Definition 4.4 (*Corresponding States*)**.** For a node $v_i \in V$, its corresponding state $Q_{v_i} \subseteq S$ is a set that holds the target states of all the corresponding transition chains of paths ending at v_i. Taking empty paths into consideration, we have $s_{init} \in Q_{v_i}$.

Note that a path $p_G \in G$ can be a subpath of other paths, which means that p_G can also correspond to one or more *sub-transition chains* that do not start with s_{init}. Nevertheless, the starting states of the sub-transition chains must belong to Q_{v_i}.

Remark (*Sub-Transition Chain*)**.** For a path p_G starting with a node v_i and being a subpath of other paths in G, each corresponding sub-transition chain of p_G must start with a state belonging to Q_{v_i}.

Example 4.1 (Corresponding States and Reachability Equivalence). Consider an instance in Figure 3 where $v_2, \cdots, v_k$ do not contain any of x or y. According to Definition 4.4, $s_x \in Q_x$. By comparing Figures 3(a) and 3(b), we can see that s_2 is obtained from s_x by two transitions $s_x \xrightarrow{\ell_{xy}} s_y \xrightarrow{\ell_2} s_2$, while s'_2 is obtained from s_x by one transition $s_x \xrightarrow{\ell_2} s'_2$. If $s_2 = s'_2$, then $s_k = s'_k$ because the sequence of edge labels $\ell_2, \ell_3, \cdots, \ell_k$ is not changed after folding (x, y). Moreover, if for any $s_x \in Q_x$, $s_2 = s'_2$, then for any p_G (Figure 3(a)) and its xy-folded $p_{G'}$ (Figure 3(b)), their corresponding transition chains end at the same state. This means that folding (x, y) keeps the paths passing through $x \xrightarrow{\ell_{xy}} y$ and their xy-folded paths consistent with respect to whether they are reachable paths.

Table 1. Edge label notations for discussing RSM-reachability.

Notation	Description
$L_{xy} = \{\ell \mid x \xrightarrow{\ell} y \in E\}$	the set of labels of the edges from x to y.
$L_{x\_} = \{\ell \mid x \xrightarrow{\ell} v_i \in E, v_i \in V\}$	the set of labels of the outgoing edges of x.
$L_{\_x} = \{\ell \mid v_i \xrightarrow{\ell} x \in E, v_i \in V\}$	the set of labels of the incoming edges of x.
$L_{\not y x} = \{\ell \mid v_i \xrightarrow{\ell} x \in E, v_i \in V, v_i \neq y\}$	the set of labels of the edges ending with x and not starting with y.
$L_{x \not y} = \{\ell \mid x \xrightarrow{\ell} v_i \in E, v_i \in V, v_i \neq y\}$	the set of labels of the edges starting with x and not ending with y.

The above example shows that, with determined Q_x and Q_y, we are able to identify whether folding (x, y) preserves reachability equivalence by computing *at most two transitions* for each state of Q_x and Q_y.

4.2 Folding Principle

Precisely computing Q_x and Q_y is equivalent to solving RSM-reachability, which is too expensive for graph folding. This section formulates our graph folding principle using an alternative overapproximation of Q_x, utilizing RSM properties, *i.e.*, *subsumption and equivalence relations* of states.

Overapproximating Q_x. With determined labels of incoming edges of x, the local states of the states in Q_x are determined. To facilitate the discussion, Table 1 lists the notations about the edge labels involving x and y. With all incoming edge labels $L_{\_x}$ of a node x in G, we collect a set of RSM local states n' with transitions $n \xrightarrow{\ell} n'$ and $\ell \in L_{\_x}$. We define the set $Nr(L_{\_x})$ as

$$Nr(L_{\_x}) = \{n' \mid n \xrightarrow{\ell} n' \in \bigcup_i \delta_i,\ \ell \in L_{\_x}\}. \tag{1}$$

Intuitively, $Nr(L_{\_x})$ holds the target RSM states whose transition labels belong to the incoming edge label set $L_{\_x}$ of x. In particular, if $x \in V_{src}$, we let $s_{init} \in Nr(L_{\_x})$. Obviously, the local states of the states in Q_x belong to $Nr(L_{\_x})$. Computing $Nr(L_{\_x})$ is very inexpensive because given $L_{\_x}$, $Nr(L_{\_x})$ can be directly determined by checking the local transition functions of the RSM. As global states are local states wrapped by layers of boxes, we have:

$$Q_x \subseteq B^* \times Nr(L_{\_x}). \tag{2}$$

Example 4.2 (Computing $Nr(L_{\_x})$). Given an RSM in Figure 4(a), Figure 4(c) is a graph segment of an RSM-reachability instance running on the RSM. In the graph segment, $L_{\_x} = \{\ell_3\}$. In the RSM, there is only one transition $n_1 \xrightarrow{\ell_3} \langle b, n_0\rangle$ labeled by ℓ_3. Thus, in Figure 4(c), $Nr(L_{\_x}) = \{\langle b, n_0\rangle\}$. Moreover, there is only one box in the RSM, i.e., $B = \{b\}$. Thus, $Q_x \subseteq \{b\}^* \times \{\langle b, n_0\rangle\}$.

In Section 4.1, we use Example 4.1 to show that we can determine whether folding (x, y) preserves reachability equivalence by computing at most two transitions for each state of Q_x and Q_y. According to Property 3.1, each transition can exit at most one box. Namely, for Q_x and Q_y, examining the states with two layers of boxes is sufficient to cover all states, as outer boxes are never affected by the two transitions. Correspondingly, while replacing Q_x by $B^* \times Nr(L_{\_x})$ and $B^* \times Nr(L_{\_y})$, examining the states of $B^\alpha \times Nr(L_{\_x})$ and $B^\alpha \times Nr(L_{\_y})$ where $\alpha \leq 2$ is enough.

Rules for Consistency. In Section 4.1, we show that ensuring reachability equivalence is to satisfy the two conditions of Definition 4.2, among which satisfying the exclusiveness condition (*Cond. 1*) is simple and addressed immediately after Definition 4.2. Here, we provide four rules in Figure 5 for

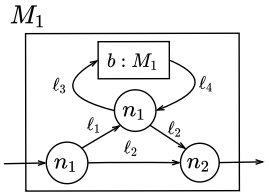

(a) An RSM.

$\langle n_0 \rangle \notin F \qquad \langle n_1 \rangle \notin F$

$L_1 = \{\ell_2\} \qquad L_2 = \{\ell_1, \ell_2\}$

$\langle n_0 \rangle \overset{L_1}{\simeq} \langle n_1 \rangle \quad \langle n_1 \rangle \overset{L_2}{\preceq} \langle n_0 \rangle \quad \langle n_0 \rangle \overset{L_2}{\not\preceq} \langle n_1 \rangle$

(b) $\preceq$ and $\simeq$ relations.

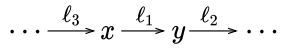

(c) Pair (x, y) is foldable.

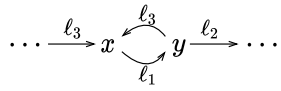

(d) Pair (x, y) is not foldable.

Fig. 4. Example of subsumption and equivalence relations of states and instances of foldable pairs (x, y).

$$\textit{Rule}\ \texttt{[x-x]}: \quad \forall s_x \xrightarrow{\ell_{xy}} s_y \xrightarrow{\ell_{yx}} s'_x \in R \ \ s.t.\ s_x \in B^\alpha \times Nr(L\_x) \bigwedge \ell_{xy} \in L_{xy} \bigwedge \ell_{yx} \in L_{yx}\ , \quad s'_x \overset{L_{x\_}}{\preceq} s_x\ .$$

$$\textit{Rule}\ \texttt{[y-y]}: \quad \forall s_y \xrightarrow{\ell_{yx}} s_x \xrightarrow{\ell_{xy}} s'_y \in R \ \ s.t.\ s_y \in B^\alpha \times Nr(L\_y) \bigwedge \ell_{xy} \in L_{xy} \bigwedge \ell_{yx} \in L_{yx}\ , \quad s'_y \overset{L_{y\_}}{\preceq} s_y\ .$$

$$\textit{Rule}\ \texttt{[x-y]}: \quad \forall s_x \in B^\alpha \times Nr(L\_x) \bigwedge \forall \ell_{xy} \in L_{xy}\ , \quad \exists s_x \xrightarrow{\ell_{xy}} s_y \in R \quad s.t.\ \ s_x \overset{L_{y\not}}{\simeq} s_y\ .$$

$$\textit{Rule}\ \texttt{[y-x]}: \quad \forall s_y \in B^\alpha \times Nr(L\_y) \bigwedge \forall \ell_{yx} \in L_{yx}\ , \quad \exists s_y \xrightarrow{\ell_{yx}} s_x \in R \quad s.t.\ \ s_y \overset{L_{x\not}}{\simeq} s_x\ .$$

Fig. 5. Rules for *Cond. 2*, where $\alpha \in \{0, 1, 2\}$, L_{xy}, $L_{x\_}$, $L_{y\not}$, and $Nr(L\_x)$ are defined in Table 1 and Eq. 1.

satisfying the consistency condition (*Cond. 2*). The four rules exploit subsumption and equivalence relations of states (Definition 4.5). Basically, the two relations are used to measure and compare the capabilities of states being transited by edge labels involving x and y.

Definition 4.5 (*Subsumption $\preceq$ and Equivalence $\simeq$ Relations of States*)**.** Given a set of labels $L \subseteq \Sigma$ and two states $s_i, s_j \in S$, s_i is subsumed by s_j with respect to L, denoted by $s_i \overset{L}{\preceq} s_j$, iff

(1) $\forall \ell \in L,\ \forall s_k \in S,\ s_i \xrightarrow{\ell} s_k \in \Delta \Rightarrow s_j \xrightarrow{\ell} s_k \in \Delta$, and (2) $s_i \in F \Rightarrow s_j \in F$.

Specifically, s_i is equivalent to s_j with respect to L, denoted by $s_i \overset{L}{\simeq} s_j$, iff $s_i \overset{L}{\preceq} s_j \bigwedge s_j \overset{L}{\preceq} s_i$.

Example 4.3. Figure 4(b) gives an example of subsumption and equivalence relations of states in the RSM of Figure 4(a). $\langle n_0 \rangle \overset{L_1}{\simeq} \langle n_1 \rangle$ because both $\langle n_0 \rangle$ and $\langle n_1 \rangle$ can transit to $\langle n_2 \rangle$ via ℓ_2. $\langle n_1 \rangle \overset{L_2}{\preceq} \langle n_0 \rangle$ because $\langle n_1 \rangle$ can transit to $\langle n_2 \rangle$ via ℓ_2 and $\langle n_0 \rangle$ can not only transit to $\langle n_2 \rangle$ via ℓ_2 but also transit to $\langle n_1 \rangle$ via ℓ_1. In contrast, $\langle n_0 \rangle \overset{L_2}{\not\preceq} \langle n_1 \rangle$ because $\langle n_0 \rangle$ can transit to $\langle n_1 \rangle$ via ℓ_1 whereas $\langle n_1 \rangle$ cannot.

Based on the two relations in Definition 4.5, we briefly discuss the rules in Figure 5. By examining the states of $B^\alpha \times Nr(L\_x)$ and the labels of incoming and outgoing edges of x and y, Rule `[x-x]` ensures the consistency of the corresponding transition chains of paths passing through x and y by starting and ending both with x. Rule `[x-y]` ensures the consistency of the corresponding transition chains of paths passing through an edge from x to y. Rules `[y-y]` and `[y-x]` are symmetric to Rules `[x-x]` and `[x-y]` with respect to x and y.

Graph Folding Principle. We provide our principle for identifying foldable (x, y) in Theorem 4.1, where Principles ① and ② are used to satisfy *Cond. 1* and *Cond. 2* of Definition 4.2, respectively. Notably, in our folding principle, each rule in Figure 5 contains no more than two transitions, and the value of α, *i.e.*, the layers of boxes, is no more than two.

Theorem 4.1 (*Graph Folding Principle*). *Consider an RSM-reachability instance Reach$\langle R, G \rangle$. Without loss of generality, assume that there is always at least one edge from node x to y in G. The node pair $(x, y) \in G$ is foldable if both ① and ② hold:*

(a) Original graph. **(b)** Incorrectly folded (x, y).

Fig. 6. For the problem running on the RSM in Figure 1(a), if $v_1 \in V_{src}$ and $v_2 \in V_{snk}$, folding (x, y) introduces an additional reachable pair (v_1, v_2) in G' via $v_1 \xrightarrow{(} x \xrightarrow{)} v_2$, which violates reachability equivalence.

① *When there is no edge from y to x, $y \notin V_{src}$ and all the incoming edges of y starts at x;*
② *The four rules in Figure 5 hold for all $\alpha \in \{0, 1, 2\}$.*

Example 4.4 (Identifying Foldable Node Pairs). Figure 4(a) is an RSM, and Figures 4 (c) and (d) are two graph segments based on the RSM. Assume that neither x nor y is a source. In Figure 4(c), there is no edge from y to x, and the only incoming edge of y starts at x, so ① is satisfied. And for ②, we only need to consider Rule [x-y]. It can be observed that $Nr(L_{\_x}) = \{\langle b, n_0\rangle\}$, $L_{xy} = \{\ell_1\}$ and $L_{y\not x} = \{\ell_2\}$. We have $\langle b, n_0\rangle \xrightarrow{\ell_{xy}=\ell_1} \langle b, n_1\rangle \in R$ and $\langle b, n_0\rangle \overset{L_{y\not x}}{\simeq} \langle b, n_1\rangle$. Therefore, the node pair (x, y) in Figure 4(c) is foldable.

In Figure 4(d), $Nr(L_{\_x}) = \{\langle b, n_0\rangle\}$, $L_{xy} = \{\ell_1\}$, $L_{yx} = \{\ell_3\}$ and $L_{y\not x} = \{\ell_2\}$. We have $\langle b, n_0\rangle \xrightarrow{\ell_{xy}=\ell_1} \langle b, n_1\rangle \xrightarrow{\ell_{yx}=\ell_3} \langle b, b, n_0\rangle \in R$ and $\langle b, b, n_0\rangle \overset{L_{\_x}}{\not\simeq} \langle b, n_0\rangle$. This means that Rule [x-x] of ② is not satisfied. Therefore, the node pair (x, y) in Figure 4(d) is not foldable.

The soundness of our graph folding principle manifests in that folding any node pair preserves reachability equivalence. Besides, since the states of $Nr(L_{yx})$ in Rule [x-y] are doubly checked by Rules [x-x] and [y-x], $Nr(L_{\_x})$ in Rule [x-y] can be replaced by $Nr(L_{\not yx})$ for simplicity. Similarly, in Rule [y-x], $Nr(L_{\_y})$ can be replaced by $Nr(L_{x\not y})$. The principle decides foldability via only local information (*i.e.*, incoming and outgoing edges of a node pair in graph G). Therefore, it does not exhaustively detect all foldable node pairs. For example, in Figure 1(b), if we only consider v_0 as the source and v_7 as the sink, folding (v_1, v_2) does not affect CFL-reachability result, whereas we do not consider it as foldable because it violates Rule [x-y] in Figure 5.

4.3 Correctness of Folding Principle

We demonstrate the correctness of our graph folding by showing that Principles ① and ② in Theorem 4.1 satisfies *Cond. 1* and *Cond. 2* in Definition 4.2, respectively. The proof is separated into proving Lemma 4.1 and Lemma 4.2, where the former is simple and intuitive. To prove Lemma 4.2, we first categorize the paths involving x and y into four basic types, as in Figure 7, and show how each rule in Figure 5 ensures the consistency of each type, respectively. This gives rise to two properties, *i.e.*, Property 4.1 and Property 4.2, which are further used to prove Lemma 4.2.

Lemma 4.1. *Principle ① in Theorem 4.1 implies the exclusiveness condition (Cond. 1) of Definition 4.2.*

Proof. A source-sink path in G' that does not have an xy-FEQ class in G can only be introduced when there is no edge from y to x, as shown in Figure 6. In this case, when $y \in V_{src}$ or y has an incoming edge from a node other than x, folding (x, y) may introduce new source-sink paths from y or the predecessors of y to x or the successors of x. Such new paths do not have any xy-FEQ class in G and can lead to spurious reachable pairs. Principle ① avoids such incorrect foldings. □

Lemma 4.2. *Principle ② in Theorem 4.1 implies the exclusiveness condition (Cond. 2) of Definition 4.2.*

	Type 1	*Type 2*	*Type 3*	*Type 4*
Original	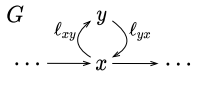	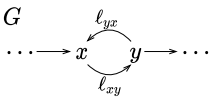	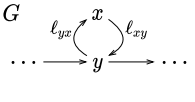	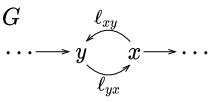
Folded	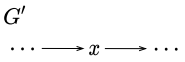	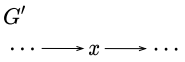	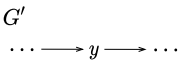	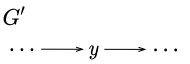
Involved rules	`[x-x]`	`[x-x]` and `[x-y]`	`[y-y]`	`[y-y]` and `[y-x]`

Fig. 7. Four basic types of xy-FEQ classes, where each type contains at most one xy-subpath. For simplicity, we only draw one edge from x to y and one edge from y to x.

We first illustrate the objectives to which the four rules take effect. Figure 7 categorizes all paths containing at most one *xy-subpath*[1] into four basic types of xy-FEQ classes, and shows the corresponding rules for ensuring consistency for each type. Briefly, Rule `[x-x]` ensures the consistency of the corresponding transition chains of paths where the xy-subpath starts and ends both with x (Type 1). Rule `[x-x]` and Rule `[x-y]` together ensure the consistency of the corresponding transition chains of paths where the xy-subpath starts with x and ends with y (Type 2). Correspondingly, `[y-y]` and `[y-x]` ensure the consistency of Type 3, where xy-subpath starts and ends both with y, and Type 4, where xy-subpath starts with y and ends with x.

Principle ② preserves the consistency for the four basic types as it has Property 4.1 and Property 4.2, among which Property 4.1 is the realization of Property 3.1 in the corresponding states of nodes, and it indicates that $B^{\alpha} \times Nr(L_x)$ and $B^{\alpha} \times Nr(L_y)$ where $\alpha = 0, 1, 2$ is enough to cover all cases (states) in Q_x and Q_y. Property 4.2 guarantees the consistency of the endpoints of transition chains corresponding to the four basic types of xy-FEQ classes, which further ensures the satisfaction of *Cond. 2*. The detailed proofs of Property 4.1 and Property 4.2 are provided in our supplementary material.

Property 4.1. If the four rules in Figure 5 hold when $\alpha \leq 2$, they also hold for all $\alpha > 2$.

Property 4.2. With $\boldsymbol{P}_{xy}$ denoting an xy-FEQ class belonging to the four basic types of Figure 7 and $p_{G'}$ denoting the xy-folded path of $\boldsymbol{P}_{xy}$, if the four rules in Figure 5 hold, then (i) $p_{G'}$ is a reachable path iff $\boldsymbol{P}_{xy}$ contains a reachable path, and (ii) when the paths of $\boldsymbol{P}_{xy}$ do not end with x or y, $p_{G'}$ corresponds to a sub-transition chain from s_0 to s_k iff $\boldsymbol{P}_{xy}$ also contains a path corresponding to a sub-transition chain from s_0 to s_k.

Proof of Lemma 4.2. We use the four basic types and the two properties to prove Lemma 4.2. In the original graph G, any path p_G can be seen as the concatenation of subpaths $p_{G1}p_{G2}\cdots p_{Gk}$ such that (1) for each $i \in \{1, \cdots, k\}$, p_{Gi} is either a path belonging to the four basic types of Figure 7 or a path not containing any xy-subpath, and (2) for all $i < k$, p_{Gi} does not end with either x or y. Discussing $k = 1$ is trivial as it either belongs to the four basic types, which is covered by Property 4.2, or is a path not containing any xy-subpath, which is never changed by folding (x, y).

Next, we consider $k > 1$ and start from p_{G1}. For the case that p_{G1} does not belong to the four basic types, the corresponding transition chain is never changed by folding (x, y), *i.e.*, the corresponding states of nodes are not changed. For the case that p_{G1} belongs to $\boldsymbol{P}_{xy_1}$ one of the four basic types in Figure 7, according to Definition 4.1, the xy-folded path $p_{G1'}$ is exactly $\boldsymbol{P}_{xy}$. Property 4.2 ensures

[1]Given two nodes x and y in a graph, an xy-path is a path comprised of edges joining x and y.

Algorithm 1: Implementation of Graph Folding Principle

```
1  Function Identify(x, y)
2      Q_x := Nr(L_x) ∪ (B × Nr(L_x)) ∪ (B^2 × Nr(L_x));
3      Q_y := Nr(L_y) ∪ (B × Nr(L_y)) ∪ (B^2 × Nr(L_y));
4      if L_yx = ∅ and (y ∈ V_src or L_x̸y ≠ ∅) then                    /* Theorem 4.1: ①  */
5          return false;
6      if Check(x, y) and Check(y, x) then                             /* Theorem 4.1: ②  */
7          return true;
8      return false;
9  Procedure Check(v_1, v_2)
10     for each s_{v_1} ∈ Q_{v_1} do
11         for each ℓ_1 ∈ L_{v_1 v_2} do
12             if not exists (s_{v_1} --ℓ_1--> s_{v_2} ∈ R s.t. s_{v_1} ≅^{L_{v_2 φ_1}} s_{v_2}) then
13                 return false;                                       /* Rules [x-y] and [y-x] of Figure 5 */
14             for each ℓ_2 ∈ L_{v_2 v_1} do
15                 if exists (s_{v_1} --ℓ_1--> s_{v_2} --ℓ_2--> s'_{v_1} ∈ R s.t. ¬(s'_{v_1} ≤^{L_{v_1 -}} s_{v_1})) then
16                     return false;                                   /* Rules [x-x] and [y-y] of Figure 5 */
17     return true;
```

that $p_{G1'}$ corresponds to a transition chain from s_{init} to s_1 iff $\boldsymbol{P}_{xy_1}$ also contains a path corresponding to a transition chain from s_{init} to s_1.

Analogously, for the concatenation $p_{G1}p_{G2}\cdots p_{Gk-1}$ that belongs to $\boldsymbol{P}_{xy_{k-1}}$, Property 4.2 ensures that the xy-folded path of $p_{G1}p_{G2}\cdots p_{Gk-1}$ (*i.e.*, of $\boldsymbol{P}_{xy_{k-1}}$) corresponds to a transition chain from s_{init} to s_{k-1} iff $\boldsymbol{P}_{xy_{k-1}}$ also contains a path corresponding to a transition chain from s_{init} to s_{k-1}.

Finally, we consider the whole path p_G, which belongs to $\boldsymbol{P}_{xy}$ and is folded into $p_{G'}$. (1) For the case that p_{G_k} does not end with x nor y, it can be inferred that $p_{G'}$ corresponds to a transition chain from s_{init} to s_k iff $\boldsymbol{P}_{xy}$ also contains a path corresponding to a transition chain from s_{init} to s_k. (2) For the case that p_G ends with x or y, Property 4.2 also ensures that $p_{G'}$ corresponds to a transition chain from s_{init} to s_k such that $s_k \in F$ iff $\boldsymbol{P}_{xy}$ also contains a path corresponding to a transition chain from s_{init} to s'_k such that $s'_k \in F$. Therefore, for any xy-FEQ class $\boldsymbol{P}_{xy}$ in G and its xy-folded path $p_{G'}$ in G', the four rules of Figure 5 ensures that $p_{G'}$ is a reachable path iff $\boldsymbol{P}_{xy}$ contains a reachable path, which indicates the satisfaction of *Cond. 2*. □

Putting Lemmas 4.1, 4.2 and Definition 4.2 together, folding a node pair (x, y) satisfying ① and ② in Theorem 4.1 preserves reachability equivalence. Namely, Theorem 4.1 is correct.

5 GRAPH-FOLDING ALGORITHM

We then give an efficient graph-folding algorithm GF that traverses and folds the input graphs for CFL-reachability. Our algorithm implements the graph folding principle (Theorem 4.1). GF has a linear time complexity with respect to the number of nodes in input graphs.

5.1 Identifying Foldable Node Pairs

5.1.1 Implementation of Graph Folding Principle. Algorithm 1 describes a practical realization of the folding principle in Theorem 4.1. The characteristic is that it only needs to compute the transitions involving the incoming and outgoing edges of a pair of adjacent nodes x and y. Specifically, in

Algorithm 2: Efficient Identification of Foldable Node Pairs

$\Omega_\oplus$: a set holding the patterns of foldable node pairs.
$\Omega_\ominus$: a set holding the patterns of non-foldable node pairs.

```
1 Function IsFoldable(x, y)
2     consult the incoming and outgoing edges to determine Pattern_(x,y);
3     if Pattern_(x,y) ∈ Ω_⊕ then return true ;
4     if Pattern_(x,y) ∈ Ω_⊖ then return false ;
5     if Identify(x, y) then                                   /* Algorithm 1 */
6         Ω_⊕ := Ω_⊕ ∪ {Pattern_(x,y)}
7         return true;
8     Ω_⊖ := Ω_⊖ ∪ {Pattern_(x,y)}
9     return false;
```

lines 2–3, we set the values of Q_x and Q_y as their overapproximate supersets according to Principle ② in Theorem 4.1. lines 4–5 and lines 6–7 verify the foldability of the input node pair based on Principles ① and ②, respectively.

Time Complexity. Algorithm 1 has a time complexity of $O(|B|^2 \times |N| \times |\Sigma|^3)$, where $N = \cup_{i\in\{1,\cdots,t\}} N_i$ is the collection of all local states of the RSM. In Algorithm 1, the time complexity of lines 2–5 can be regarded as $O(1)$ as they can be considered as lookups of hash tables. Then, the time complexity of Algorithm 1 depends on the subprocedure `Check`. We can first assume that a state transition $s_i \xrightarrow{t} s_j \in R$ can be performed in $O(1)$ time. According to Definition 4.5, given a set of label L and two states s_1 and s_2, checking $s_1 \overset{L}{\cong} s_2$ and $s_1 \overset{L}{\preceq} s_2$ needs to perform $O(|L|)$ transitions. Thus, the loops in lines 10–16 cost $(|Q_{v_1}|\times|L_{v_1v_2}|\times|L_{v_2\not v_1}|+|Q_{v_1}|\times|L_{v_1v_2}|\times|L_{v_2v_1}|\times|L_{v_1\_}|)$ time, where the value of Q_{v_1} is given in line 2 or line 3. We can find that $O(|Q_{v_1}|) = O(|B|^2 \times |N|)$, $|L_{v_1v_2}| \le |\Sigma|$, $|L_{v_2\not v_1}| \le |\Sigma|$, $|L_{v_2v_1}| \le |\Sigma|$ and $|L_{v_1\_}| \le |\Sigma|$. Therefore, the time complexity of Algorithm 1 is $O(|B|^2 \times |N| \times |\Sigma|^3)$.

5.1.2 Efficient Identification for Foldable Node Pairs. Algorithm 1 runs fast for small RSMs, but the overall runtime increases when the RSMs become more complex. For real-world problems, we need a more efficient identification strategy. In fact, real-world CFL-reachability problems usually have an important trait—many node pairs share the same "pattern" of incoming and outgoing edges. Specifically, we define the "pattern" of a node pair (x, y) as a tuple:

$$Pattern_{(x,y)} = \langle \texttt{isSrc}(x),\ \texttt{isSrc}(y),\ L_{\not yx},\ L_{x\not y},\ L_{xy},\ L_{yx},\ L_{x\not y},\ L_{y\not x}\rangle \tag{3}$$

where $\texttt{isSrc}(x)$ and $\texttt{isSrc}(y)$ are two boolean variables denoting whether $x \in V_{src}$ and whether $y \in V_{src}$. The value of $Pattern_{(x,y)}$ can be predefined or determined by consulting x and y and their incoming and outgoing edges. Obviously, for two node pairs (x_1, y_1) and (x_2, y_2), checking whether $Pattern_{(x_1,y_1)} = Pattern_{(x_2,y_2)}$ is much faster than calling Algorithm 1 twice.

For the node pairs sharing the same pattern $Pattern_{(x,y)}$, we do not need to repeatedly invoke Algorithm 1 to check whether they are foldable. We use a set denoted by $\Omega_\oplus$ to collect the patterns of node pairs that are already identified as foldable by Algorithm 1. When $\Omega_\oplus$ is fully filled, we can identify whether a node pair is foldable by checking whether the pattern of the node pair is already in $\Omega_\oplus$. $\Omega_\oplus$ can be filled by verifying each possible pattern through Algorithm 1, where the number of invocation depends only on the size of the alphabet Σ. Besides, we provide another strategy in Algorithm 2, which dynamically constructs $\Omega_\oplus$ during the process of graph folding with a set $\Omega_\ominus$ holding patterns of non-foldable node pairs.

Algorithm 3: Graph-Folding Algorithm GF

$V_{visited}$: a set holding visited nodes.
$E_{visited}$: a set holding visited edges.
1 **Function** GF(G, R)
2 set $\Omega_{\oplus}$, $\Omega_{\ominus}$, $V_{visited}$ and $E_{visited}$ as $\emptyset$;
3 **for** each $x \in V$ **do**
4 **if** $x \notin V_{visited}$ **then** Visit(x); ;
5 **return** G;
6 **Procedure** Visit(x)
7 $V_{visited} := V_{visited} \cup \{x\}$
8 **for** each $x \xrightarrow{\ell} y \in E\ s.t.\ y \notin V_{visited}$ and $x \xrightarrow{\ell} y \notin E_{visited}$ **do**
9 add all edges joining x and y into $E_{visited}$;
10 **if** IsFoldable(x, y) **then**
11 Fold(x, y);
12 Visit(y)
13 **Procedure** Fold(x, y)
14 Remove all edges joining x and y;
15 **for** each $z \in V\ s.t.\ Rep(z) = y$ **do** /* Update representative nodes */
16 $Rep(z) := x$;
17 Remove node y; /* Merge y into x */

5.2 Overall Algorithm

Algorithm 3 describes the overall graph-folding algorithm GF. In addition to $\Omega_{\oplus}$ and $\Omega_{\ominus}$ in Algorithm 2, Algorithm 3 maintains two sets $V_{visited}$ and $E_{visited}$ to collect the visited nodes and edges. The procedures GF and Visit scan the input graph via a depth-first traversal. When visiting a node x, the algorithm calls the identification procedure isFoldable for each unvisited direct successor y of x to check whether (x, y) is foldable. If (x, y) is foldable, the algorithm uses Fold(x, y) in lines 13–17 to fold (x, y) and update representative nodes.

Complexity. Algorithm 3 has a linear time complexity with respect to the number of nodes in the input graph. For real-world problems where the RSM is far smaller than the graph, the cost for identifying and folding a node pair (lines 10–11) can be considered as $O(1)$ time. The ordinary depth-first traversal costs $O(|V| + |E|)$ time. However, different from the ordinary depth-first traversal, line 9 ensures that each node should not be visited twice through different edges. Lines 8–12 show that the number of method invocations for IsFoldable(x, y) and Fold(x, y) does not exceed the number of visited nodes. In Algorithm 3, each node is visited once, hence the time complexity of Algorithm 3 is $O(k|V|)$ where k is a constant representing the time for identifying and folding a node pair. Namely, GF has a linear time complexity with respect to the number of nodes of the input graph.

6 EXPERIMENTS

We evaluate our graph-folding algorithm GF by applying it to two popular client analyses for C/C++: value-flow analysis [Sui et al. 2014] and alias analysis [Zheng and Rugina 2008]. In particular, we study the performance of GF from two aspects: (1) the performance of GF in reducing the input graph sizes and (2) the speedups and memory overhead reductions for CFL-reachability, with the input graphs simplified by GF.

$$S ::= call_i\ S\ ret_i \mid S\ S \mid a^*$$

(a) Value-flow analysis.

$$M ::= \overline{d}\ V\ d$$
$$V ::= (M?\ \overline{a})^*\ V\ (a\ M?)^* \mid \overline{f_i}\ V\ f_i \mid M?$$

(b) Alias analysis.

Fig. 8. CFGs for context-sensitive value-flow analysis and field-sensitive alias analysis.

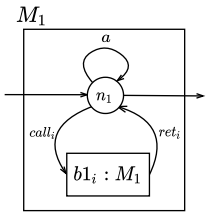

(a) Value-flow analysis.

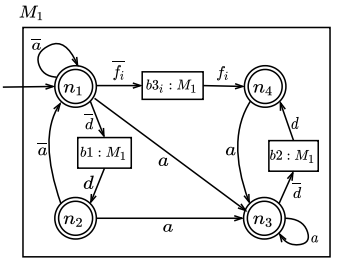

(b) Alias analysis. The doubly-circled nodes denote the exits of M_1.

Fig. 9. RSMs for context-sensitive value-flow analysis and field-sensitive alias analysis.

In summary, the experimental results are promising. On average, by reducing 60.96% nodes and 42.67% edges of the input graphs, Gf accelerates context-sensitive value-flow analysis by 4.65× with a memory reduction rate of 57.35%; by reducing 38.93% nodes and 35.61% edges, Gf accelerates field-sensitive alias analysis by 3.21× with a memory reduction rate of 65.19%. Gf is also well-compatible with existing techniques. The combination of Gf with SCC [Nuutila and Soisalon-Soininen 1994] and InterDyck [Li et al. 2020] reduces up to 72.26% and 58.85% edges from the input graph of context-sensitive value-flow analysis and field-sensitive alias analysis, respectively, accelerating the analyses by at most 9.70× and 6.30×.

6.1 Experimental Setup

We have implemented Gf on top of LLVM-12.0.0, and conducted our experiments on a platform consisting of an eight-core 2.60 GHz Intel Xeon CPU with 128 GB memory, running Ubuntu 18.04. In our experiments, the patterns of foldable node pairs, *i.e.*, $\Omega_\oplus$ in Section 5.1.2, are precomputed.

Grammar Selection. We evaluate graph folding based on two client analyses, a context-sensitive value-flow analysis [Sui et al. 2014] and a field-sensitive alias analysis [Zheng and Rugina 2008]. Figure 8 gives the corresponding context-free grammars. Both grammars extend Dyck languages with regular languages, which are representative of many CFL-reachability-based program analyses. In particular, Dyck languages have been extensively used to model function calls/returns, references/dereferences, and field writes/reads [Kodumal and Aiken 2004]. Regular languages have been used to model control/value flows. Moreover, the two client analyses have also been evaluated in existing work [Lei et al. 2022; Wang et al. 2017]. Figure 9 gives the corresponding RSM representations.

Value-flow Analysis. We conduct context-sensitive value-flow analyses on sparse value-flow graphs (SVFGs) [Sui et al. 2014]. The RSM for context-sensitive value-flow analysis is displayed in Figure 9(a), where "$call_i$" and "ret_i" denote call and return of a callsite, whose index is i; and "a" denotes an assignment instruction. In the RSM, the initial state and the final state are both $\langle n_1 \rangle$, and the unique box b has a subscript i, matching the index of $call_i$ and ret_i. In this reachability problem, nodes denoting the allocation/deallocation sites are marked as sources/sinks. It is worthwhile to

Table 2. Benchmark info and results of the baseline CFL-reachability solver, POCR [Lei et al. 2022]. #Node and #Edge denote the numbers of nodes and edges of each input graph, respectively. P-Edge% denotes the percentage of parenthesis edges out of the total edges of each input graph. Time/s and Mem./GB denote the runtime and memory overhead of the baseline for analyzing each program, measured in seconds and gigabytes, respectively.

Bench.	*Value-flow analysis*					*Alias analysis*				
	#Node	#Edge	P-Edge%	Time/s	Mem./GB	#Node	#Edge	P-Edge%	Time/s	Mem./GB
1.astyle	227140	394839	16.58%	2914	107.72	70906	150090	45.84%	172	8.01
2.git_checkout	488092	919390	37.65%	49643*	4.55*	78801	184734	42.05%	2052	61.51
3.i3	145259	212761	29.96%	36	4.69	39894	95620	43.57%	223	9.62
4.janet	227081	359552	33.10%	1218	35.06	43837	99292	43.17%	498	13.53
5.mruby	226528	340374	19.18%	26679*	2.43*	71265	176888	43.17%	2437	77.14
6.nvim	332733	402753	21.75%	15	2.35	99826	224170	43.18%	1327	69.65
7.opencv_test_video	385060	509439	10.47%	23	4.65	132068	279528	40.13%	534	18.58
8.psql	157014	228604	27.43%	131	13.78	40145	99164	44.59%	223	9.25
9.redis-cli	231372	367291	34.59%	72	12.32	55250	129528	45.45%	547	27.76
10.tmux	243828	390084	29.11%	182	10.35	76522	186808	45.63%	1676	91.90

∗ The results marked by * are obtained by Graspan [Wang et al. 2017] because POCR ran out of memory.

point out that although the RSM in Figure 9(a) only focuses on context-sensitivity, the analysis is field-sensitive because each field object in SVFGs is already represented as a distinct node.

Alias Analysis. Figure 9(b) gives the RSM for all-pair field-sensitive alias analyses, where all nodes are considered as both sources and sinks. In the RSM, a denotes an assignment, d denotes a pointer dereference, and f_i denotes the address of the i-th field. The RSM contains three boxes $b1, b2$, and $b3$, which are all mapped to M_1. $b3$ has a subscript i matching the field index of $\overline{f_i}$ and f_i. The RSM has an initial state $\langle n_1 \rangle$ and four accepting states $\langle n_1 \rangle$, $\langle n_2 \rangle$, $\langle n_3 \rangle$ and $\langle n_4 \rangle$. The alias analysis is conducted on program expression graphs (PEGs), which are bidirected, *i.e.*, for each $v_i \xrightarrow{t} v_j \in E$ where $t \in \Sigma$, there is a reverse $v_j \xrightarrow{\overline{t}} v_i \in E$.

Benchmarks. We selected ten popular GitHub open-source C/C++ programs to benchmark our analysis in Table 2. We chose these programs because they are diverse in terms of functionalities as they include: development (`astyle`, `nvim`), version control (`git-checkout`), compiler (`janet`, `mruby`), database (`psql`, `redis_cli`), computer vision (`opencv_test_video`), window manager (`i3`) and terminal multiplexer (`tmux`). The SVFG and PEG of each program are generated by the open-source tool SVF [Sui and Xue 2016b] from the bitcode files compiled by Clang-12.0.0 with the `-O3` flag and integrated by Whole Program LLVM.[2]

Evaluated Algorithms. Our graph-folding algorithm Gf is a preprocessing technique for speeding up CFL-reachability. Therefore, in our evaluation, we need to choose a baseline CFL-reachability algorithm (for solving CFL-reachability). To this end, we select two recent CFL-reachability solvers, Graspan [Wang et al. 2017] and POCR [Lei et al. 2022]. In general, POCR runs faster than Graspan. Therefore, we pick POCR [Lei et al. 2022] as the baseline CFL-reachability solver. However, POCR ran out of memory on two benchmark programs `git_checkout` and `mruby`. For both programs, we used Graspan to obtain the results. Table 2 displays the graph statistics and the results of the baseline approach. We compare our graph-folding algorithm Gf against two existing preprocessing techniques: cycle elimination (SCC) [Nuutila and Soisalon-Soininen 1994; Tarjan 1972] and graph

[2] https://github.com/travitch/whole-program-llvm.

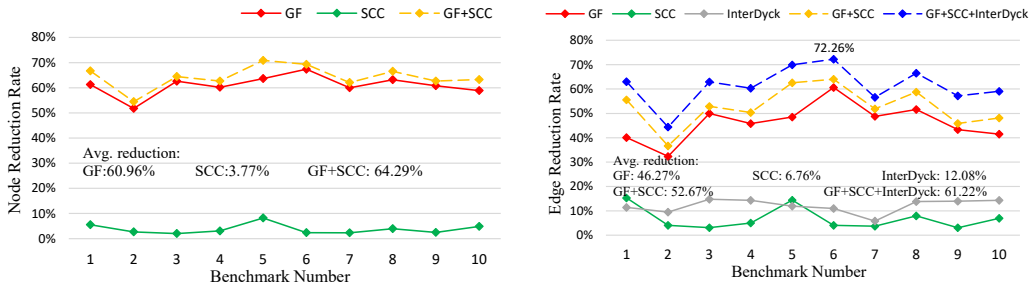

(a) Node reduction. **(b)** Edge reduction.

Fig. 10. Reduction rates of nodes and edges in the input graphs of value-flow analysis.

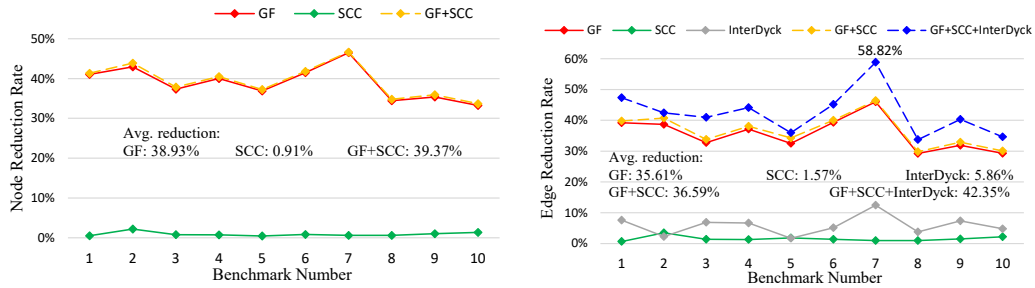

(a) Node reduction. **(b)** Edge reduction.

Fig. 11. Reduction rates of nodes and edges in the input graphs of alias analysis.

simplification for interleaved Dyck-reachability (InterDyck) [Li et al. 2020]. For each input graph, SCC detects and collapses cycles comprised of a-edges, and InterDyck detects and eliminates the non-Dyck-contributing parenthesis edges. Note that, unlike Gf, neither SCC nor InterDyck is a general technique for CFL-reachability.

Evaluation of Correctness. To ensure correctness, we check whether the baseline CFL-reachability solver can compute equivalent solutions from the original input graph G and the simplified version G', which is folded from G by Gf. Specifically, for each program, after obtaining the solutions from G and G', we expand all reachable pairs comprised of representative nodes (v'_i, v'_j) in G' into $\{(v_i, v_j) \mid Rep(v_i) = v'_i, Rep(v_j) = v'_j\}$, and comparing the reachable pairs with the solutions on G. Our comparison demonstrates that the expanded solutions on the folded graphs are identical to the solutions on the original graphs.

6.2 Performance in Reducing Graph Sizes

Figures 10 and 11 depict the reduction rates of nodes and edges in the input graphs of value-flow analysis and alias analysis, respectively. As InterDyck does not remove nodes from a graph, the node reduction charts (Figure 10(a) and Figure 11(a)) do not include the information of InterDyck. A comparison of SCC, InterDyck and Gf shows that Gf is more efficient than SCC and InterDyck in reducing the size of the input graphs for both clients. Specifically, by comparing Gf with SCC, we find that cycle elimination reduces only a small number of nodes and edges in the preprocessing stage. Prior work shows that cycle elimination works well in constraint-based pointer analysis because the edges typically denote subset constraints [Hardekopf and Lin 2007a; Pereira and Berlin

Table 3. Runtime of GF, SCC and InterDyck, measured in seconds.

Bench.	*Value-flow analysis*			*Alias analysis*		
	GF	SCC	InterDyck	GF	SCC	InterDyck
1.astyle	3.70	0.69	273.04	0.29	0.13	19.82
2.git_checkout	15.29	2.09	1625.84	0.40	0.21	337.87
3.i3	2.63	0.27	177.74	0.54	0.05	45.96
4.janet	4.01	0.80	464.37	0.19	0.07	27.41
5.mruby	15.74	0.82	718.08	0.44	0.15	257.75
6.nvim	16.72	0.94	152.02	0.44	0.31	122.89
7.opencv_test_video	57.80	2.35	541.36	0.55	0.47	22.54
8.psql	2.39	0.30	130.31	0.29	0.05	37.56
9.redis-cli	7.34	0.64	143.18	0.21	0.14	85.16
10.tmux	10.13	0.75	1040.18	0.32	0.16	216.08

2009]. However, in CFL-reachability, the edges in the input graph are labeled with different letters. By comparing GF with InterDyck, we find that InterDyck can reduce the number of parenthesis edges. But because the proportions taken by parenthesis edges are not large (see Columns 4 and 9 of Table 2) in these two real-world clients, whereby the effectiveness of InterDyck is limited. Besides, a comparison between node reduction rates and edge reduction rates of GF shows that folding tends to increase the density (#Edge/#Node) of the graph.

We also study the combinations GF+SCC and GF+SCC +InterDyck, which are depicted as the dashed lines in Figures 10 and 11. The result shows that GF complements SCC and InterDyck well, *i.e.*, they can be used together to further improve the performance of CFL-reachability. Table 3 shows the runtime of GF, SCC and InterDyck when they are applied separately to the graphs. The results show that SCC is the fastest, followed by GF, and InterDyck is much slower. This is because implementing InterDyck in these two clients needs to (1) detect and contract all non-parenthesis edges, (2) use the FastDyck algorithm [Zhang et al. 2013] to find Dyck-contributing edges and mark the "anchor" nodes and (3) detect and remove non-Dyck-contributing edges, where (1) costs $O(|V|^2)$ time, (2) costs $O(|V| + |E|\log|E|)$ time and (3) costs $O(|E|\log|E|)$ time.

6.3 Speedup and Memory Overhead

Figure 12 shows the speedups of CFL-reachability by GF, SCC, InterDyck, and their combinations. Taking the edge reduction rate (Figure 10(b) and Figure 11(b)) into consideration and comparing the speedups among different graph simplification approaches, we observe that the reduction of more edges from the graphs helps to improve CFL-reachability solving. Comparing the speedups of a graph simplification approach among different programs, we can see that larger edge reduction rates usually, but not always, result in larger speedups. This is because the runtime of CFL-reachability solving depends not only on the size of the input graph but also on other graph traits, such as density and edge types.

Figure 13 shows the reduction rates of memory overheads by GF in the two client analyses. Comparing the performance of `git_checkout` and `mruby` (solved by Graspan) with other benchmarks (solved by POCR) in Figure 13(a), we can see that the memory overhead reduction by GF for POCR is much more significant than for Graspan. This is also observable in Figure 13(b), where all benchmarks are solved by POCR. The insight is that when solving CFL-reachability, POCR maintains a spanning tree for each node to hold the "transitive" edges (*i.e.*, *a*-edges) for the graphs. Reducing the nodes and edges in the graph also reduces the auxiliary spanning trees, leading to those dramatic reduction rates of memory overhead. A comparison of Figure 12 and Figure 13 indicates that, in general, larger speedups correspond to larger memory overhead reductions. What

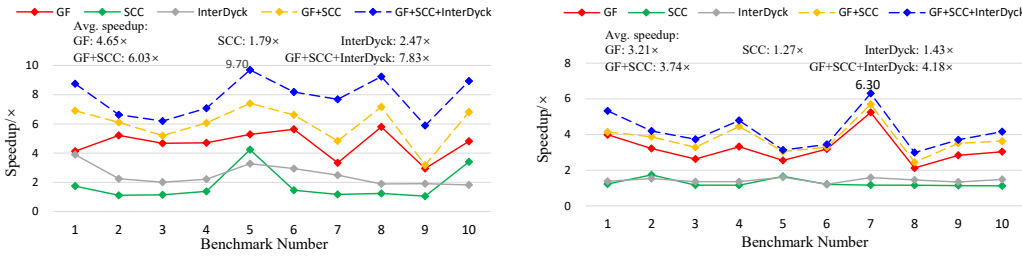

(a) Context-sensitive value-flow analysis. **(b)** Field-sensitive alias analysis.

Fig. 12. Speedups of CFL-reachability by GF, SCC, InterDyck and their combinations.

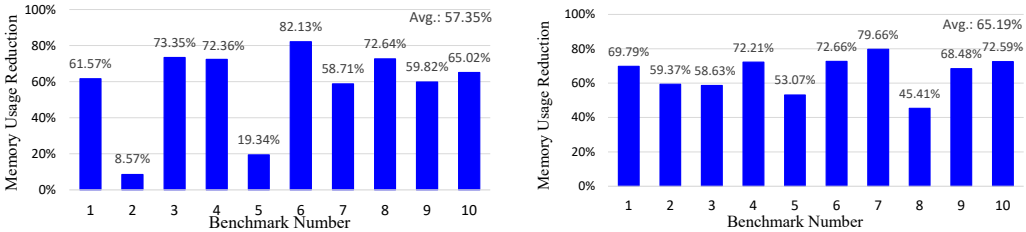

(a) Context-sensitive value-flow analysis. **(b)** Field-sensitive alias analysis.

Fig. 13. Reduction rates of memory overhead by GF.

lies behind this correlation is that solving CFL-reachability is adding new edges to the graph according to existing edges. Therefore, a larger speedup means a larger reduction rate of edges that need to be created and stored. This ultimately reduces the memory overhead.

6.4 Discussions

Graph Folding and Domain-Specific Edge Contraction. Perhaps the best-known domain-specific edge contraction technique in static analysis is the offline variable substitution (OVS) for pointer analysis [Rountev and Chandra 2000]. Specifically, OVS can contract a *copy*-edge from a node x to another node y if y does not have its address taken and y does not have any other incoming *copy*-edge. In our evaluated alias analyses, GF folds a node pair (x, y) where there is an a-edge from x to y if y does not have any incoming d-edge and f_i-edge, and does not have any incoming a-edge not from x. The intrinsic meaning of the folding condition of GF is equivalent to that of OVS.[3] Thus, OVS can be viewed as an instantiation of graph folding in pointer/alias analysis.

Foldability of Node Pairs v.s. Self-Loops in the RSM. By observing the RSMs of the two clients of our experiments (Figures 9(a) and 9(b)), a common feature is that both RSMs contain self-loops, *e.g.*, $n_1 \xrightarrow{a} n_1$ in the RSM of Figure 9(a). It is interesting to note that a foldable node pair does not necessarily need to be joined by an edge that corresponds to a self-loop in the RSMs. Consider the node pair (x, y) in Figure 4(c), whose foldability is discussed in Example 4.4. In the example, the edge $x \xrightarrow{\ell_1} y$ does not correspond to a self-loop in the RSM of Figure 4(a). In fact, the RSM in this example does not contain any self-loop.

Choosing Sources and Sinks. In our value-flow analysis experiments, we chose allocation/deallocation sites as sources/sinks on SVFGs (Section 6.1), following the original memory leak detection [Sui

[3]In particular, an f_i-edge is regarded as a *copy*-edge with an offset i in field-sensitive analysis [Pearce et al. 2007].

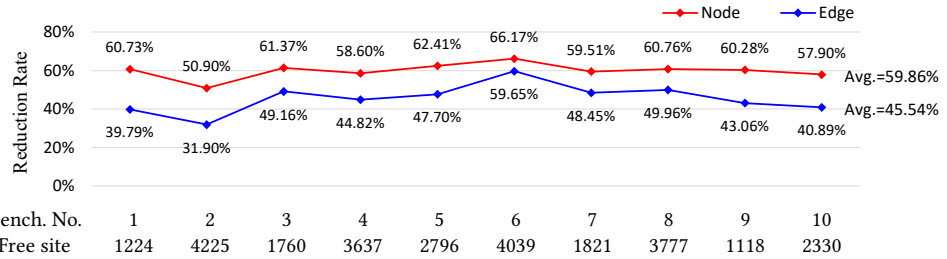

Fig. 14. Reduction rates of nodes and edges by GF, for double-free value-flow analysis on the 10 benchmarks.

et al. 2014]. To further demonstrate the effectiveness of our approach, we perform an additional double-free analysis by choosing source-sink pairs different from the memory leak detection application. The double-free problem on SVFGs can also be seen as a source-sink reachability problem by reusing the grammar in Figure 8(a) and the RSM in Figure 9(a). A simplified version of the analysis requires that each allocated memory must be freed at most once when traversing SVFGs. Specifically, any deallocation site of variable p should never reach any other deallocation sites of variable q, where p and q are aliases. As a result, we choose deallocation sites as both the source and sink in our simplified double-free analysis, in which each deallocation *free(p)* on SVFGs is treated as a store instruction assigning an *nullptr* to the location that *p* points to. Figure 14 gives the number of deallocation sites and the reduction rates of nodes and edges by GF for each benchmark. We can see that GF can achieve similar reduction rates with a different set of sources and sinks. Compared with the original value-flow analysis (Figure 10), the reduction rates in Figure 14 are slightly lower, and the difference is roughly the number of free sites. This is because the sources in the simplified double-free analysis usually have incoming *a*-edges. The node pairs involving such edges cannot be folded by GF, but are foldable in the value-flow analysis for memory leak detection.

7 RELATED WORK

Due to the (sub)cubic time complexity of CFL-reachability with respect to the input graph size, improving the practical performance of CFL-reachability is desirable. However, the truly subcubic CFL-reachability algorithms [Le Gall 2014; Williams and Williams 2018] are impractical due to the large constant. In the literature, significant progress has been made only for specific clients or particular context-free grammars [Bastani et al. 2015; Chatterjee et al. 2018; Yan et al. 2011; Zhang et al. 2013, 2014; Zheng and Rugina 2008].

Due to the impracticability of reducing the time complexity of CFL-reachability, reducing the size of the input graph has been studied and adopted by many researchers. The most prevalent technique is cycle elimination [Nuutila and Soisalon-Soininen 1994; Tarjan 1972], which has been widely applied to an alternative form of CFL-reachability, *i.e.*, constraint solving [Fähndrich et al. 1998; Hardekopf and Lin 2007a; Kodumal and Aiken 2004; Pereira and Berlin 2009; Xu et al. 2009]. What limits the applicability of cycle elimination in CFL-reachability is that whether a cycle can be merged depends on the context-free grammar. Edge contraction has also been studied for domain-specific clients [Hardekopf and Lin 2007b; Rountev and Chandra 2000]. Such methods can be seen as specializations of our graph folding in these clients. Recently, Li et al. [2020] proposed an algorithm to remove the non-Dyck-contributing edges for interleaved-Dyck-reachability problems. The approach only focuses on reducing redundant parenthesis edges, but there are also numerous non-parenthesis edges to be eliminated in real-world problems.

Reducing the redundancy of on-the-fly CFL-reachability solving is also studied by researchers [Bravenboer and Smaragdakis 2009; Jordan et al. 2016; Lei et al. 2022; Wang et al. 2017].

These techniques are orthogonal with our GF, and they can be applied together to solve a CFL-reachability problem. CFL-reachability is also studied in two alternative forms called (1) recursive state machines (RSMs) [Alur et al. 2005b, 2006; Benerecetti et al. 2010; Chatterjee et al. 2015; Chatterjee and Velner 2012; Chaudhuri 2008], and (2) pushdown automata (PDA) [Chatterjee and Velner 2012; Reps et al. 2007, 2005; Rytter 1983; Späth et al. 2019; Wojciech and Rytter 1985]. Several approaches are proposed to simplify visibly pushdown automata (VPA) [Gauwin et al. 2019; Heizmann et al. 2017]. By exploiting the equivalence property of states, Heizmann et al. [2017] simplify visibly pushdown automata (VPA) to make a complex automaton simple. Prior work shows that the minimization of VPA is NP-complete by reducing the minimizing immersions problem to the problem of minimizing VPA [Gauwin et al. 2019]. These techniques are also orthogonal to our graph folding, as they focus on simplifying the CFL itself rather than the graph.

8 CONCLUSION

This paper has described a new graph folding technique for CFL-reachability. It has formulated the criteria for foldable node pairs and proposed a graph-folding algorithm GF. Experimental results of context-sensitive value-flow analysis and field-sensitive alias analysis for C and C++ on ten open-source programs show substantial performance improvements enabled by GF via reducing the graph sizes. On average, GF reduces 60.96% of nodes and 42.67% of edges of the input graphs for value-flow analysis, obtaining a speedup of 4.65× and a memory usage reduction of 57.35%, and reduces 38.93% of nodes and 35.61% of edges of the input graphs for alias analysis, obtaining a speedup of 3.21× and a memory usage reduction of 65.19%.

DATA AVAILABILITY STATEMENT

Materials for our evaluation are publicly available [Lei et al. 2023] and can be used to reproduce the data of our experiment. The code is sourced from the project https://github.com/kisslune/POCR.

ACKNOWLEDGMENT

We would like to thank the anonymous reviewers and the shepherd Peisen Yao for valuable feedback on earlier drafts of this paper, which helped improve its presentation. This research is supported by Australian Research Grants DP210101348 and FT220100391; by Amazon under an Amazon Research Award in automated reasoning; by the United States National Science Foundation (NSF) under grants No. 1917924 and No. 2114627; and by the Defense Advanced Research Projects Agency (DARPA) under grant N66001-21-C-4024. Any opinions, findings, and conclusions or recommendations expressed in this publication are those of the authors and do not necessarily reflect the views of the above sponsoring entities.

REFERENCES

Rajeev Alur, Michael Benedikt, Kousha Etessami, Patrice Godefroid, Thomas Reps, and Mihalis Yannakakis. 2005a. Analysis of recursive state machines. *ACM Transactions on Programming Languages and Systems (TOPLAS)* 27, 4 (2005), 786–818. https://doi.org/10.1145/1075382.1075387

Rajeev Alur, Swarat Chaudhuri, Kousha Etessami, and P Madhusudan. 2005b. On-the-fly reachability and cycle detection for recursive state machines. In *International Conference on Tools and Algorithms for the Construction and Analysis of Systems*. Springer, 61–76. https://doi.org/10.1007/978-3-540-31980-1_5

Rajeev Alur, Salvatore La Torre, and P Madhusudan. 2006. Modular strategies for recursive game graphs. *Theoretical computer science* 354, 2 (2006), 230–249. https://doi.org/10.1016/j.tcs.2005.11.017

Rajeev Alur and Parthasarathy Madhusudan. 2004. Visibly pushdown languages. In *Proceedings of the thirty-sixth annual ACM symposium on Theory of computing*. 202–211. https://doi.org/10.1145/1007352.1007390

Osbert Bastani, Saswat Anand, and Alex Aiken. 2015. Specification Inference Using Context-Free Language Reachability. *Acm Sigplan Notices* 50, 1 (2015), 553–566. https://doi.org/10.1145/2775051.2676977

Massimo Benerecetti, Stefano Minopoli, and Adriano Peron. 2010. Analysis of timed recursive state machines. In *2010 17th International Symposium on Temporal Representation and Reasoning*. IEEE, 61–68. https://doi.org/10.1145/1075382.1075387

Martin Bravenboer and Yannis Smaragdakis. 2009. Strictly declarative specification of sophisticated points-to analyses. In *Proceedings of the 24th ACM SIGPLAN conference on Object oriented programming systems languages and applications*. 243–262. https://doi.org/10.1145/1639949.1640108

Krishnendu Chatterjee, Bhavya Choudhary, and Andreas Pavlogiannis. 2018. Optimal Dyck reachability for data-dependence and alias analysis. *Proc. ACM Program. Lang.* 2, POPL (2018), 30:1–30:30. https://doi.org/10.1145/3158118

Krishnendu Chatterjee, Rasmus Ibsen-Jensen, Andreas Pavlogiannis, and Prateesh Goyal. 2015. Faster algorithms for algebraic path properties in recursive state machines with constant treewidth. In *Proceedings of the 42nd Annual ACM SIGPLAN-SIGACT Symposium on Principles of Programming Languages*. 97–109. https://doi.org/10.1145/2676726.2676979

Krishnendu Chatterjee and Yaron Velner. 2012. Mean-payoff pushdown games. In *2012 27th Annual IEEE Symposium on Logic in Computer Science*. IEEE, 195–204. https://doi.org/10.1109/LICS.2012.30

Swarat Chaudhuri. 2008. Subcubic algorithms for recursive state machines. In *Proceedings of the 35th annual ACM SIGPLAN-SIGACT symposium on Principles of programming languages*. 159–169. https://doi.org/10.1145/1328897.1328460

Manuel Fähndrich, Jeffrey S Foster, Zhendong Su, and Alexander Aiken. 1998. Partial online cycle elimination in inclusion constraint graphs. In *Proceedings of the ACM SIGPLAN 1998 conference on Programming language design and implementation*. 85–96. https://doi.org/10.1145/277652.277667

Olivier Gauwin, Anca Muscholl, and Michael Raskin. 2019. Minimization of visibly pushdown automata is NP-complete. *arXiv preprint arXiv:1907.09563* (2019). https://doi.org/10.48550/arXiv.1907.09563

Tang Hao, Xiaoyin Wang, Lingming Zhang, Xie Bing, Zhang Lu, and Mei Hong. 2015. Summary-Based Context-Sensitive Data-Dependence Analysis in Presence of Callbacks. In *Acm Sigplan-sigact Symposium on Principles of Programming Languages*. https://doi.org/10.1145/2676726.2676997

Ben Hardekopf and Calvin Lin. 2007a. The ant and the grasshopper: fast and accurate pointer analysis for millions of lines of code. In *Proceedings of the 28th ACM SIGPLAN Conference on Programming Language Design and Implementation*. 290–299. https://doi.org/10.1145/1273442.1250767

Ben Hardekopf and Calvin Lin. 2007b. Exploiting pointer and location equivalence to optimize pointer analysis. In *International Static Analysis Symposium*. Springer, 265–280. https://doi.org/10.1007/978-3-540-74061-2_17

David L. Heine and Monica S. Lam. 2003. A practical flow-sensitive and context-sensitive C and C++ memory leak detector. (2003), 168. https://doi.org/10.1145/780822.781150

Matthias Heizmann, Christian Schilling, and Daniel Tischner. 2017. Minimization of visibly pushdown automata using partial Max-SAT. In *International Conference on Tools and Algorithms for the Construction and Analysis of Systems*. Springer, 461–478. https://doi.org/10.48550/arXiv.1701.05160

Herbert Jordan, Bernhard Scholz, and Pavle Subotić. 2016. Soufflé: On synthesis of program analyzers. In *International Conference on Computer Aided Verification*. Springer, 422–430. https://doi.org/10.1007/978-3-319-41540-6_23

John Kodumal and Alex Aiken. 2004. The set constraint/CFL reachability connection in practice. *ACM Sigplan Notices* 39, 6 (2004), 207–218. https://doi.org/10.1145/996893.996867

François Le Gall. 2014. Powers of tensors and fast matrix multiplication. In *Proceedings of the 39th international symposium on symbolic and algebraic computation*. 296–303. https://doi.org/10.1145/2608628.2608664

Yuxiang Lei, Shin Hwei Sui, Tan, and Qirun Zhang. 2023. Artifact of "Recursive State Machine Guided Graph Folding for Context-Free Language Reachability". https://doi.org/10.5281/zenodo.7708433

Yuxiang Lei and Yulei Sui. 2019. Fast and precise handling of positive weight cycles for field-sensitive pointer analysis. In *International Static Analysis Symposium*. Springer, 27–47. https://doi.org/10.1007/978-3-030-32304-2_3

Yuxiang Lei, Yulei Sui, Shuo Ding, and Qirun Zhang. 2022. Taming transitive redundancy for context-free language reachability. *Proceedings of the ACM on Programming Languages* 6, OOPSLA2 (2022), 1556–1582. https://doi.org/10.1145/3563343

Yuanbo Li, Qirun Zhang, and Thomas Reps. 2020. Fast graph simplification for interleaved Dyck-reachability. In *PLDI '20: 41st ACM SIGPLAN International Conference on Programming Language Design and Implementation*. https://doi.org/10.1145/3385412.3386021

David Melski and Thomas Reps. 2000. Interconvertibility of a class of set constraints and context-free-language reachability. *Theoretical Computer Science* 248, 1-2 (2000), 29–98. https://doi.org/10.1145/258994.259006

Nomair A Naeem and Ondrej Lhoták. 2008. Typestate-like analysis of multiple interacting objects. *ACM Sigplan Notices* 43, 10 (2008), 347–366. https://doi.org/10.1145/1449764.1449792

Esko Nuutila and Eljas Soisalon-Soininen. 1994. On finding the strongly connected components in a directed graph. *Inform. Process. Lett.* 49, 1 (1994), 9–14. https://doi.org/10.1016/0020-0190(94)90047-7

David J Pearce, Paul HJ Kelly, and Chris Hankin. 2007. Efficient field-sensitive pointer analysis of C. *ACM Transactions on Programming Languages and Systems (TOPLAS)* 30, 1 (2007), 4–es. https://doi.org/10.1145/1290520.1290524

Fernando Magno Quintao Pereira and Daniel Berlin. 2009. Wave propagation and deep propagation for pointer analysis. In *2009 International Symposium on Code Generation and Optimization*. IEEE, 126–135. https://doi.org/10.1109/CGO.2009.9

Jakob Rehof and Manuel Fähndrich. 2001. Type-base flow analysis: from polymorphic subtyping to CFL-reachability. *ACM SIGPLAN Notices* 36, 3 (2001), 54–66. https://doi.org/10.1145/373243.360208

Thomas Reps, Susan Horwitz, and Mooly Sagiv. 1995. Precise interprocedural dataflow analysis via graph reachability. In *Proceedings of the 22nd ACM SIGPLAN-SIGACT symposium on Principles of programming languages*. 49–61. https://doi.org/10.1145/199448.199462

Thomas Reps, Akash Lal, and Nick Kidd. 2007. Program analysis using weighted pushdown systems. In *International Conference on Foundations of Software Technology and Theoretical Computer Science*. Springer, 23–51. https://doi.org/10.1007/978-3-540-77050-3_4

Thomas Reps, Stefan Schwoon, Somesh Jha, and David Melski. 2005. Weighted pushdown systems and their application to interprocedural dataflow analysis. *Science of Computer Programming* 58, 1-2 (2005), 206–263. https://doi.org/10.1016/j.scico.2005.02.009

Thomas W. Reps. 1998. Program analysis via graph reachability. *Information & Software Technology* 40, 11-12 (1998), 701–726. https://doi.org/10.1016/S0950-5849(98)00093-7

Atanas Rountev and Satish Chandra. 2000. Off-line variable substitution for scaling points-to analysis. *Acm Sigplan Notices* 35, 5 (2000), 47–56. https://doi.org/10.1145/349299.349310

Wojciech Rytter. 1983. Time complexity of loop-free two-way pushdown automata. *Inform. Process. Lett.* 16, 3 (1983), 127–129. https://doi.org/10.1016/0020-0190(83)90063-7

Johannes Späth, Karim Ali, and Eric Bodden. 2019. Context-, flow-, and field-sensitive data-flow analysis using synchronized Pushdown systems. *Proc. ACM Program. Lang.* 3, POPL (2019), 48:1–48:29. https://doi.org/10.1145/3291641

Yulei Sui, Xiao Cheng, Guanqin Zhang, and Haoyu Wang. 2020. Flow2Vec: value-flow-based precise code embedding. *Proceedings of the ACM on Programming Languages* 4, OOPSLA (2020), 1–27. https://doi.org/10.1145/3428301

Yulei Sui and Jingling Xue. 2016a. On-demand strong update analysis via value-flow refinement. In *Proceedings of the 2016 24th ACM SIGSOFT international symposium on foundations of software engineering*. 460–473. https://doi.org/10.1145/2950290.2950296

Yulei Sui and Jingling Xue. 2016b. SVF: interprocedural static value-flow analysis in LLVM. In *Proceedings of the 25th international conference on compiler construction*. 265–266. https://doi.org/10.1145/2892208.2892235

Yulei Sui and Jingling Xue. 2018. Value-flow-based demand-driven pointer analysis for C and C++. *IEEE Transactions on Software Engineering* 46, 8 (2018), 812–835. https://doi.org/10.48550/arXiv.1701.05650

Yulei Sui, Ding Ye, and Jingling Xue. 2014. Detecting memory leaks statically with full-sparse value-flow analysis. *IEEE Transactions on Software Engineering* 40, 2 (2014), 107–122. https://doi.org/10.1145/2338965.2336784

Robert Tarjan. 1972. Depth-first search and linear graph algorithms. *SIAM journal on computing* 1, 2 (1972), 146–160. https://doi.org/10.1137/0201010

Kai Wang, Aftab Hussain, Zhiqiang Zuo, Guoqing Xu, and Ardalan Amiri Sani. 2017. Graspan: A single-machine disk-based graph system for interprocedural static analyses of large-scale systems code. *ACM SIGARCH Computer Architecture News* 45, 1 (2017), 389–404. https://doi.org/10.1145/3093336.3037744

Virginia Vassilevska Williams and R. Ryan Williams. 2018. Subcubic Equivalences Between Path, Matrix, and Triangle Problems. *J. ACM* 65, 5 (2018), 27:1–27:38. https://doi.org/10.1145/3186893

Wojciech and Rytter. 1985. Fast recognition of pushdown automaton and context-free languages. *Information and Control* (1985). https://doi.org/10.1016/S0019-9958(85)80024-3

Guoqing Xu, Atanas Rountev, and Manu Sridharan. 2009. Scaling CFL-reachability-based points-to analysis using context-sensitive must-not-alias analysis. In *European Conference on Object-Oriented Programming*. Springer, 98–122. https://doi.org/10.1007/978-3-642-03013-0_6

Dacong Yan, Guoqing Xu, and Atanas Rountev. 2011. Demand-driven context-sensitive alias analysis for Java. In *Proceedings of the 2011 International Symposium on Software Testing and Analysis*. 155–165. https://doi.org/10.1145/2001420.2001440

Qirun Zhang, Michael R Lyu, Hao Yuan, and Zhendong Su. 2013. Fast algorithms for Dyck-CFL-reachability with applications to alias analysis. In *Proceedings of the 34th ACM SIGPLAN conference on Programming language design and implementation*. 435–446. https://doi.org/10.1145/2491956.2462159

Qirun Zhang and Zhendong Su. 2017. Context-sensitive data-dependence analysis via linear conjunctive language reachability. In *Proceedings of the 44th ACM SIGPLAN Symposium on Principles of Programming Languages*. 344–358. https://doi.org/10.1145/3093333.3009848

Qirun Zhang, Xiao Xiao, Charles Zhang, Hao Yuan, and Zhendong Su. 2014. Efficient subcubic alias analysis for C. In *Proceedings of the 2014 ACM International Conference on Object Oriented Programming Systems Languages & Applications*. 829–845. https://doi.org/10.1145/2660193.2660213

Xin Zheng and Radu Rugina. 2008. Demand-driven alias analysis for C. In *Proceedings of the 35th annual ACM SIGPLAN-SIGACT symposium on Principles of programming languages*. 197–208. https://doi.org/10.1145/1328897.1328464